Alexander Mokina, BSc

Thermoanalysis of the debinding process of ceramic multilayer components

MASTER'S THESIS

to achieve the university degree of

Diplom-Ingenieur

Master's degree programme: Technical Chemistry

submitted to

Graz University of Technology

Supervisor

Klaus Reichmann, Ao.Univ.-Prof. Dipl.-Ing. Dr.techn.

Institute for Chemistry and Technology of Materials (ICTM)

Graz, January 2021

AFFIDAVIT

I declare that I have authored this thesis independently, that I have not used other than the declared sources/resources, and that I have explicitly indicated all material which has been quoted either literally or by content from the sources used. The text document uploaded to TUGRAZonline is identical to the present master's thesis.

Date, Signature

Abstract

Ceramic capacitors are widely used in the fields of modern electronics. They are built up in a multilayered architecture with alternating layers of ceramic material and an inner metal electrode. The so called Multilayer Ceramic Capacitor (MLCC) plays an important role in all kinds of electronics. Just recently they are also found in high power applications such as high power microwaves or hybrid electric vehicles. The manufacturing of these MLCCs is a complex process and starts with the production of ceramic tapes by a casting process. These ceramic tapes contain a huge variety of different organic additives, which are responsible for the flexibility and processability of the ceramic mixture. However, these organics have to be removed prior to the subsequent manufacturing steps. This specific process step, the so called organic burnout or binder burnout, is very important, because it can cause many quality relating problems if carried out not careful enough. Furthermore this process step is very time consuming and can last for several days. This is a problem and the reason why it is investigated closely within this thesis. The results showed that, depending on the oxygen partial pressure, different side reactions like oxidation of the inner metal electrode or reduction of the ceramic material were occurring. By changing the atmosphere and/or the temperature during the heat treatment it could be achieved that either one or the other (oxidation of the metal electrode or reduction of the ceramic material) was prevented. However, it is very difficult to prevent both simultaneously. Even with a modified setup of changing the atmosphere and the temperature during the process, the side reactions could not be prevented completely.

Kurzfassung

Keramische Kondensatoren sind in modernen elektronischen Anwendungen weit verbreitet. Sie sind mehrschichtig, mittels abwechselnder Schichten aus keramischem Material und Metallelektroden, aufgebaut. Der keramische Vielschichtkondensator (Multilayer Ceramic Capacitor - MLCC) spielt eine wichtige Rolle in nahezu allen Bereichen der Elektronik, in jüngster Zeit auch bei Hochleistungsanwendungen wie beispielsweise Hochleistungsmikrowellen oder Hybrid-Elektrofahrzeugen. Die Herstellung dieser MLCCs ist ein komplexer Prozess und beginnt mit der Herstellung der Keramikfolien, dem sogenannten Folienziehen. Die Keramikfolien enthalten dafür eine Vielzahl von organischen Zusatzstoffen um eine ausreichende Flexibilität und Verarbeitbarkeit der Keramikmischung zu gewährleisten. Diese Zusatzstoffe müssen jedoch vor den darauffolgenden Herstellungsschritten wieder entfernt werden. Dieser Prozessschritt ist sehr wichtig, da es bei unsachgemäßer Durchführung zu Qualitätsproblemen der Bauteile kommen kann. Darüber hinaus ist dieser Schritt sehr zeitintensiv und kann mehrere Tage in Anspruch nehmen. Dies ist ein großes Problem und der Grund für die genauen Untersuchungen dieses Produktionsabschnittes im Rahmen dieser Arbeit. Es zeigte sich, dass je nach Sauerstoffpartialdruck, unterschiedliche Nebenreaktionen wie beispielsweise Oxidation der Innenelektrode oder Reduktion des keramischen Materials auftreten. Durch Verändern der Atmosphäre und/oder der Temperatur während des Prozesses konnte entweder das eine oder das andere (Oxidation der Elektrode oder Reduktion des keramischen Materials) verhindert werden. Es ist jedoch sehr schwierig beide Nebenreaktionen gleichzeitig zu verhindern. Selbst bei modifizierten Bedingungen und wechselnden Atmosphären- beziehungsweise Temperatureinstellungen während der Messung, konnten die Nebenreaktionen nicht vollständig verhindert werden.

Danksagung

An dieser Stelle möchte ich allen Danken die mich während dem Verfassen dieser Arbeit unterstützt und begleitet haben.

Zuallererst möchte ich mich vielmals bei Herrn Prof. Klaus Reichmann für seine, zu jeder Zeit offenen Ohren, seinen unermüdlichen Bemühungen und seiner Geduld bedanken. Vor allem dafür, immer erreichbar gewesen zu sein wenn es Probleme gab oder ich Fragen hatte. Vielen Dank für eine so nette und freundliche Begleitung während dieser Arbeit.

Besonderer und aufrichtiger Dank gilt zudem dem Unternehmen TDK in Deutschlandsberg, vor allem Herrn Dr. Alexander Glazunov, Herrn Dr. Denis Orosel und Frau Dr. Marion Ottlinger, die diese Arbeit überhaupt erst ermöglicht haben. Vielen Dank für Ihre Unterstützung.

Zudem möchte ich all meinen Studienkollegen, vor allem aber Anne, Daniel, Maximilian, Richard und Tobias für ihre Unterstützung, aber vor allem für eine unvergessliche Studienzeit danken. Vielen Dank auch an Martin für seine Hilfe.

Großer Dank gebührt außerdem meiner ganzen Familie für die moralische und finanzielle Unterstützung während meiner gesamten Studienzeit.

Danke Marlene, dass du mich immer motiviert und unterstützt hast.

x

Contents

List of Illustrations

Figures

Tables

List of Acronyms and Symbols

MLCC – Multilayer Ceramic Capacitor

PLZT – Lanthanum doped Lead Zirconate Titanate

STA – Simultaneous Thermal Analysis

MS – Mass Spectrometry

XRD – X-Ray Diffraction

DSC – Differential Scanning Calorimetry

TG – Thermogravimetric analysis

DSC – Differential scanning calorimetry

SIM mode (in MS measurements) – Selected ion monitoring

T_{max} – Maximum temperature during a measurement

1 Introduction

The possibility to store electrical energy is very important for various kinds of electronic applications. The most commonly used component on printed circuit boards, which meets this requirement is the multilayer capacitor[1]. Because of their fast charge-discharge capability, multilayer capacitors have very high energy densities compared to electrochemical energy storage devices, e.g. batteries. Therefore they are often used for high power applications and are mostly made of ceramics or polymers[2]. Ceramic capacitors are mainly realized via a multilayered architecture, which means that alternating layers of ceramic material and metallic electrodes are building up the capacitors. The production of these so called Multilayer Ceramic Capacitors (MLCC) includes complex manufacturing steps, with one of them being the removal of organic additives that were required in the ceramic mixture in earlier production steps. However, this step can cause huge problems concerning the part quality. If carried out not careful enough, the reaction products of the process (evolving gases) can damage the components and lead to a reduced performance of the final product. Depending on the part size and the settings of the process (mild/harsh conditions), this production step can be expected to take up to several days[3]. Therefore it has a high optimization potential and is subject of interest. This thesis takes a closer look on this specific production step and the mechanisms behind the process of debindering. In the following, the investigated components are described in more detail.

1.1 Subject of Investigation

The subject of investigation is shown in Figure 1 **(a)**. It is a ceramic multilayer component in the "green" state (just after the forming process) with the ceramic being Lanthanum doped Lead Zirconate Titanate (PLZT), inner electrodes that are made of copper and a wide variety of organic additives that are necessary for multilayer manufacturing. A schematic representation with a cross section of the parts is shown in Figure 1 **(b)**. The size of the component is approximately 1cm x 1cm x 0.4cm and it is produced via a tape casting process, which is discussed in more detail in Chapter

<center>(a)   (b)</center>
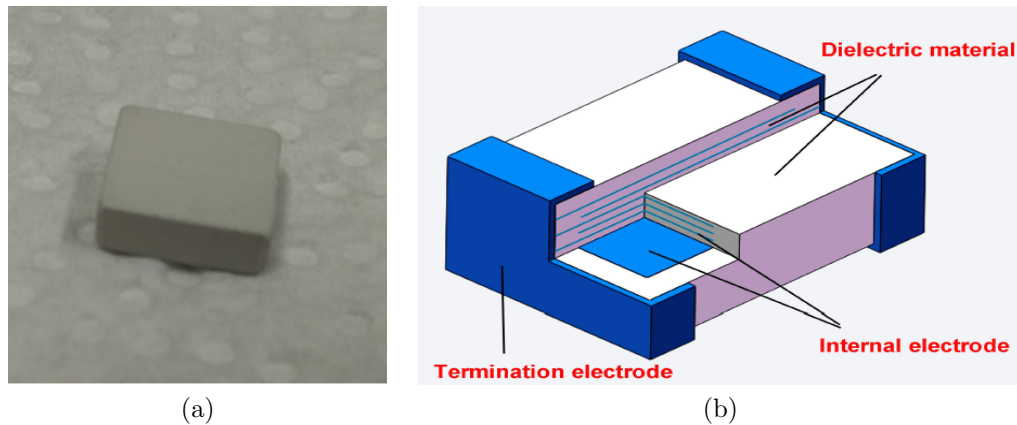
Figure 1: **(a)** Picture of the component that is investigated within this thesis.
(b) Schematic representation of the investigated component. It shows the layered structure of the parts, which is achieved via alternating layers of ceramic material and the inner metal electrodes[4].

1.2.1. The advantage of the tape casting process is that the resulting Multilayer Ceramic Capacitors (MLCCs) have higher energy storage densities than ceramics that are produced as plate or tube capacitors[2]. This is due to a smaller layer thickness that can be achieved with this type of manufacturing.

The solid solution $Pb_x La_{1-x}(Zr_{y-1}Ti_y)O_3$ is used in a wide field of electronic applications due to its polarization properties (e.g. piezoelectric material)[2][5]. Furthermore PLZT can be adapted for specific applications and desired mechanical and electric properties by changing the composition and the alloying additives[6]. Generally a piezoelectric material can either give an electric signal when it is under a mechanical deformation (direct piezoelectric effect) or it can deform itself under the influence of an electric field (indirect piezoelectric effect). Therefore these materials are an excellent choice for several electrical applications such as e.g. sensors, actuators, filters and more[7].

1.2 Manufacturing of Multilayer Ceramic Capacitors

The components that are investigated within this thesis (Figure 1 **(a)**) are produced starting with the tape casting process. It is a technique that produces ceramic tapes, which are then used to produce multilayer components via postprocessing steps. The tape casting process is discussed in more detail in the following chapter.
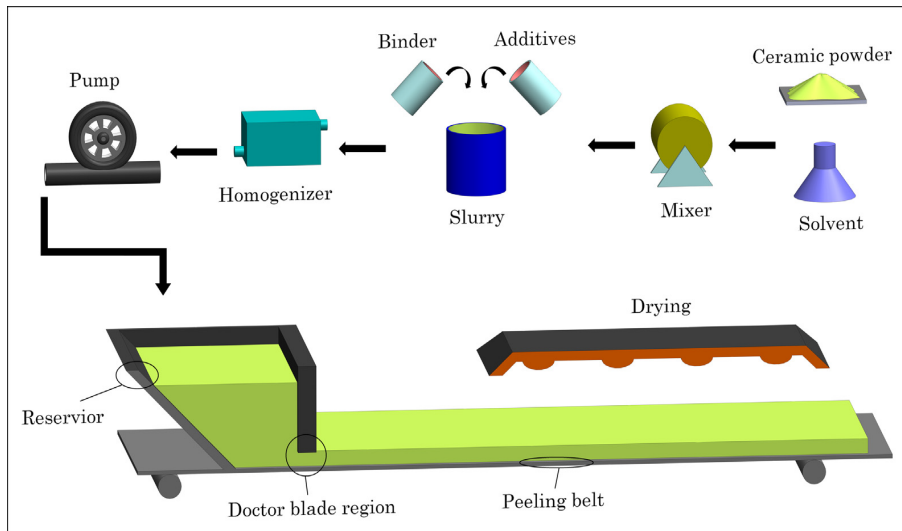
Figure 2: Schematic representation of the tape casting process. The start is in the top right corner, where the ceramic powder is mixed with a solvent. After adding polymeric compounds for better processing, the so called slurry is filled into a reservoir and then drawn via the peeling belt to the desired thickness. The thickness of the resulting ceramic tape can be varied with the doctor blade and it is then dried afterwards[8].

1.2.1 Tape casting process

1.2.1.1 General aspects

Tape casting was first used around the 1940s and is sometimes also called the doctor-blade process[8]. This is the case because the doctor-blade is the crucial part of this process as it determines the thickness of the resulting ceramic tape. A schematic representation of the process is shown in Figure 2. It starts with the mixing of the ceramic powder with a solvent (top right of Figure 2). Then, organic additives are added to the slurry, which is then transferred into a reservoir. The doctor-blade region determines the thickness of the resulting ceramic tape, which is drawn via the peeling belt. This results in ceramic tapes of up to hundreds of meters in length and thicknesses ranging from $1\mu m$ to $3000\mu m$[8].

1.2.1.2 Slurry composition and processing

Due to easier processing, e.g. powder dispersion and slurry drying, non-aqueous slurries are preferably used for the tape casting process[9]. Due to health and environmental reasons, aqueous slurries can be used as an alternative to organic solvent based ones[9][10]. However, the disadvantage of these slurries is the high sensitivity to process variations

and an overall complex multiphase system[10]. As shown in Figure 2, the mixing and homogenizing (dispersion) steps are normally realized with a two-stage milling process. In the first step the powder, solvent and a dispersant are mixed for about 12-24 hours. Only after this the binder and plasticizers are added and the mixture is again mixed for another 2-24 hours. This split of the mixing steps is necessary in order to guarantee a complete homogenization while preventing a possible degradation of the high molecular weight binder molecules[9].

1.2.1.3 Casting and drying

For the casting process itself, the homogeneously mixed slurry is transferred into a reservoir, which is important to ensure that the ceramic tape can be drawn continuously via the peeling belt. The thickness of the resulting ceramic tape is determined by the gap between the doctor blade and the peeling belt, the larger the distance between the two parts the thicker is the resulting tape. Furthermore, the speed of the peeling belt and the drying shrinkage has an influence of the resulting thickness of the tape[9]. The tape itself is normally cast on a clean, smooth, insoluble surface, e.g. cellulose acetate, Teflon® or Mylar®[9]. Drying of the ceramic tape is generally achieved by moving the tape through a drying tunnel. This leads to solvent vaporization and consequently to a viscoelastic tape[9].

1.2.2 Ceramic multilayer technology

The ceramic tape, which is manufactured via the tape casting process (green frame in Figure 3), is mainly used to produce Multilayer Ceramic Capacitors (MLCCs). For this, the flexible ceramic tape is cut into rectangular pieces and the electrodes are printed on them by screen printing of metal pastes. Many layers (up to a hundred or more) of the tape are stacked and laminated together. This package is then cut into equally sized parts[8]. In order to get usable ceramic parts, the components ("green bodies" at this stage) must then undergo a subsequent process step that is called firing, which proceeds in three steps: (1) organic burnout (=binder burnout) (2) the actual sintering step (3) cooling[3]. The binder burnout is generally achieved at temperatures between 250°C-500°C.

The red frame in Figure 3 shows the step in the production of a MLCC that is the subject of investigation throughout this thesis, namely the binder burnout. It is a crucial step, because the oxygen partial pressure has to be controlled in such a way,

4
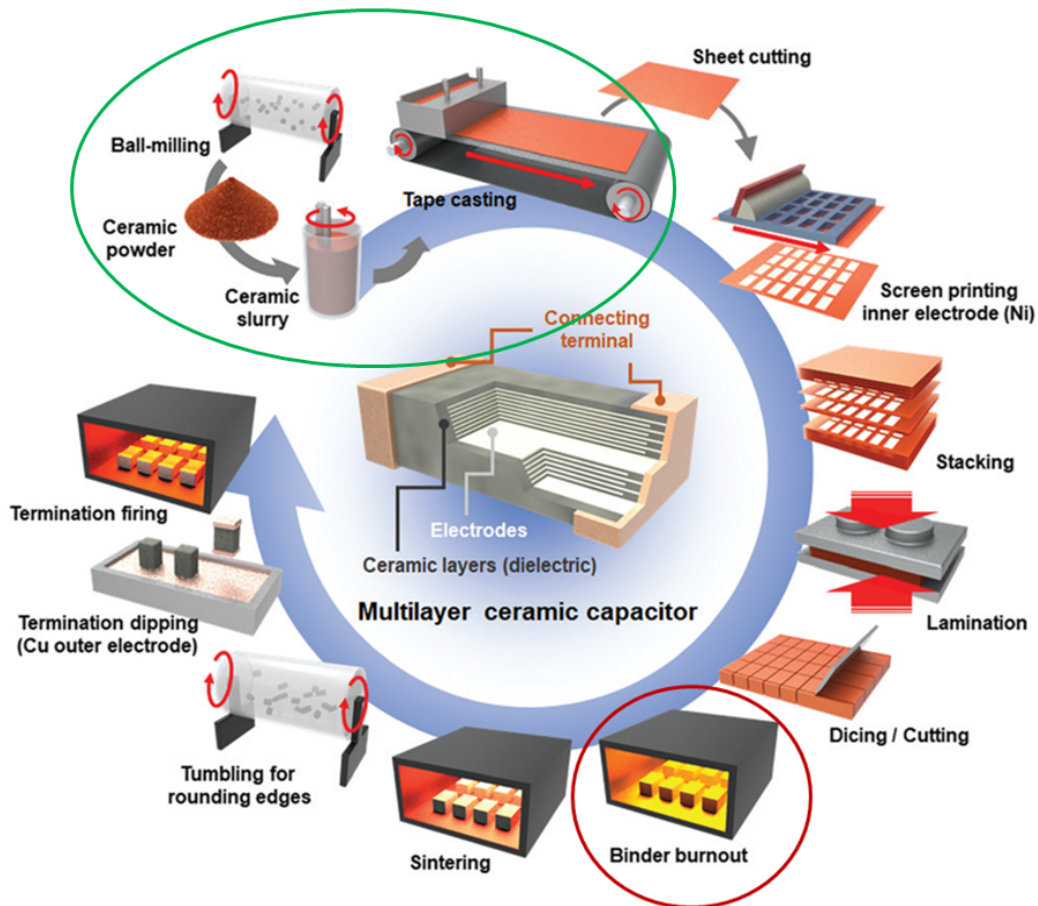
Figure 3: Schematic representation of the production of a multilayer ceramic capacitor (MLCC). The green frame indicates the tape casting process, which is explained in more detail in chapter 1.2.1. All processes after that (printing of the inner electrodes, stacking, lamination, cutting, binder burnout, sintering and so on) are leading to the final product – the MLCC. The red frame shows the step of the production, which is subject of investigation throughout this thesis, namely the binder burnout[11].

that the inner electrode is not oxidized and the ceramic material is not reduced and therefore decomposed. This is discussed in more detail in Chapter 1.3.2 (Side reactions) and Chapter 3 (Results and Discussion). However, the binder burnout is a necessary step prior to the sintering process. Otherwise the polymer burnout would happen way too fast during the densification process and this in turn would result in mechanical failures of the material, e.g. cracks on the surface.

1.3 Task

Due to the high importance and optimization potential of the binder burnout process step, it is the central point of interest throughout this thesis. The overall goal is a thermogravimetric investigation of the debinding process in different atmospheres, the analysis of volatile reaction products during the debinding process and how a change of the oxygen partial pressure affects the outcome of this process step. For this, preliminary investigations with flakes of the final components were carried out to get a rough idea of how the material reacts in different atmospheres. After that, components with and without inner electrodes were used to identify the differences in the reactivity. Different atmosphere means different oxygen partial pressures, depending on the gas mixture that was chosen for the respective experiment. This is described in more detail in Chapter 2.3.

1.3.1 Thermolysis (Binder burnout)

A good overview of the content of this chapter can be found in the literature[3].

In addition to the binder burnout other reactions may also occur during this presintering heat treatment, e.g. vaporization of water or thermolysis of organic materials that were introduced as contaminants during the tape casting process. It is crucial that this step is carried out carefully, as evolving gas that is generated by thermolysis can cause cracks on the surface of the components and therefore would damage the product. This means that a proper choice of the binder, the correct temperature, controlled heating and a suitable atmosphere are very important to achieve reasonable results. Furthermore the binder burnout, or oxidative degradation in general, is limited by oxygen diffusion and therefore the product size. This means that, due to a shorter diffusion distance, binder molecules that are near the surface of the component are removed faster than binder molecules that are located near the center of the component[12]. In more reductive atmospheres (lower oxygen partial pressure), e.g. N_2 or forming gas, the oxidation of the binder is limited and may only occur because of adsorbed oxygen or oxygen in the binder molecules. Therefore vaporization is the predominant mechanism of the thermolysis in these types of atmospheres and it is shifted to higher temperatures. Furthermore, due to the reduced oxygen partial pressure, residual carbon can be expected inside the components. This residual carbon is assumed to correspond to the carbon backbone of the binder molecules, which would require higher oxygen partial pressures and/or higher temperatures to be removed from the material. The evolving carbon is assumed

to mainly correspond to the side chains of the binder molecules as they are easier to be cleaved off.

Other reactions of the material, e.g. oxidation of the copper electrode or reduction of the ceramic, are termed "side-reactions" in the following, as they are undesired and cause problems regarding the product quality.

1.3.2 Side reactions

The before mentioned residual carbon, that may remain in the components if the thermolysis is carried out in atmospheres with reduced oxygen partial pressures (more reducing atmospheres), can cause undesired side reactions. Together with the low oxygen partial pressure it can generate carbon monoxide (CO) in the pores of the components[3]. This CO is reactive and can change the stoichiometry of the ceramic material[3] (reduction of the material). It is assumed that metallic Pb is most likely be formed via reduction as the other constituents of the ceramic (Zr, Ti and La) are more stable against reduction.

If the oxygen partial pressure is increased (e.g. 0.5%, 1% and 5% O_2) this phenomenon does not occur. However, due to the reason that the inner electrodes of the components are made of copper, an oxidation of those may happen. Depending on the oxygen partial pressure and the temperature two oxidation products, namely Cu_2O and CuO, are possible.

Both types of side reaction (reduction of the ceramic and oxidation of the inner copper electrode) are undesired and can damage the components to a certain degree. In order to identify the side reactions, when they are occuring and at which specific conditions (atmosphere and temperature) they are most prominent, the measurements were carried out with two different types of components. First, components without inner electrodes were used to get a closer look on the reduction reactions of the ceramic. Components with inner electrodes were then used to investigate the oxidation reactions of the copper.

1.3.3 Methodology

A combination of a Simultaneous Thermal Analysis (STA) and a Mass Spectrometer (MS) was used to investigate the behaviour of the components during the heat treatment. Additionally X-Ray Diffraction (XRD) was helpful to identify the occuring side reaction products.

2 Experimental

The matrix of the investigated component is rather complex and consists of several constituents. Furthermore the parts are built up in layers of different materials, which can also affect the debinding process (binder burnout). For that reason, all constituents have to be considered in the investigation of these ceramic components. In the following section these different constituents are described in more detail.

2.1 Materials

2.1.1 Ceramic - Lanthanum doped Lead Zirconate Titanate (PLZT)

The ceramic that is used for the production of the investigated parts is Lanthanum doped Lead Zirconate Titanate (PLZT). It is one of the most studied antiferroelectric materials in the fields of energy storage and has an energy density of 6.4 J/cm^3[2].

2.1.2 Organic additives

2.1.2.1 Binder - Polyvinyl butyral, Polyvinyl alcohol, Polyvinyl acetate

Organic additives are a very important part of the green body. These additives, which are mostly polymers, ensure that the mechanical properties of the mixture fit the respective manufacturing process step, e.g. tape casting. Furthermore they improve the particle packing, provide lubrication between the particles and increase the strength of the green body[13]. The polymeric binder, which is part of the investigated components, is a mixture of Polyvinyl butyral, Polyvinyl alcohol and Polyvinyl acetate. Its chemical structure is shown in Figure 4. Polyvinyl butyral is a widely used organic additive in the fields of ceramics processing[14]. It is an acetal, which is synthesized from the reaction of an aldehyde and an alcohol. Structure A in Figure 4 shows the Polyvinyl butyral, structure B shows the Polyvinyl alcohol and structure C shows the Polyvinyl acetate. The used binder is a mixture of these three building blocks A, B and C and
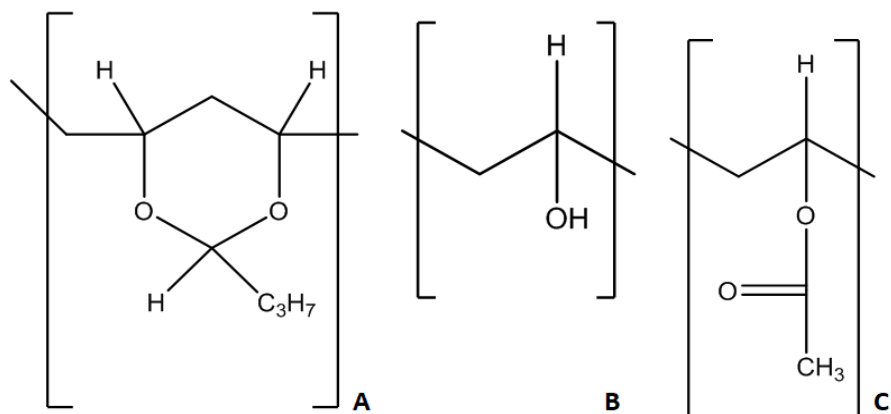
Figure 4: Chemical structure of the components of the binder.

the properties of the binder varies depending on the ratio of them[15]. It remains in the formed ceramic body (green body) until the binder burnout step during the multilayer manufacturing.

2.1.2.2 Plasticizer (Oxydipropyl dibenzoate)

Another organic additive that is present in the investigated component is shown in Figure 5. It acts as a plasticizer, which means that it makes the polymer materials softer and more flexible[16]. This is very important in the production of a multilayer component via a tape casting process.
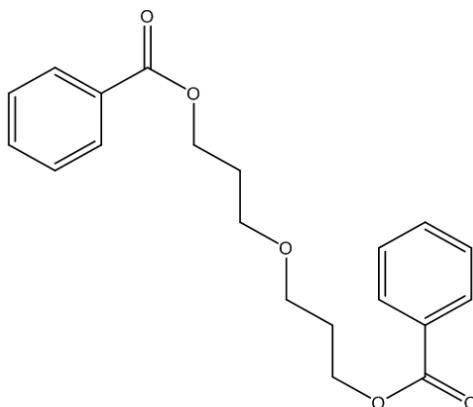
Figure 5: Chemical Structure of the plasticizer.

2.1.3 Internal electrode

2.1.3.1 Copperpaste

The investigated ceramic components are used in electric devices and therefore contain inner electrodes to realize a parallel capacitor array. These electrodes are made of copper, and in the production step, a copper paste is applied by screen printing on the ceramic tape to form them. The copper paste itself contains pure copper powder and a variety of different organic additives, which were not disclosed by the supplier in detail. These additives have to be considered in the investigation of the debinding process of the whole component. Furthermore the copper itself is of high interest due to possible oxidation and therefore volume expansion, which could occur during the debinding process. This is a source of mechanical and electrical failure of the whole component. In order to understand what happens exactly during the debinding process, the copperpaste has been investigated separately from the ceramic material. To do so, the paste was put on an watch glass and then dried for 1h at 170°C, as shown in Figure 6. The dried paste was then scraped off the glass and the flakes were treated in the same way as the whole ceramic component.
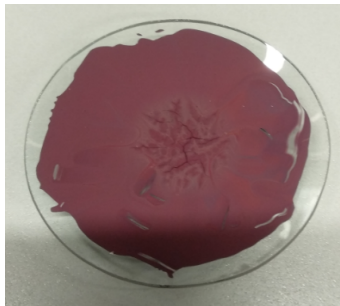
Figure 6: Dried copper paste on a watch glass.

2.2 Methods

2.2.1 STA - Simultaneous Thermal Analysis

For the studies of this thesis the STA was chosen. It is a type of thermogravimetric analysis (TG) that can measure thermal and mass change effects simultaneously. A TG in general measures the mass change of a specimen as a function of the temperature, mostly under vacuum or a specific atmosphere (e.g. pure O_2, N_2)[17].
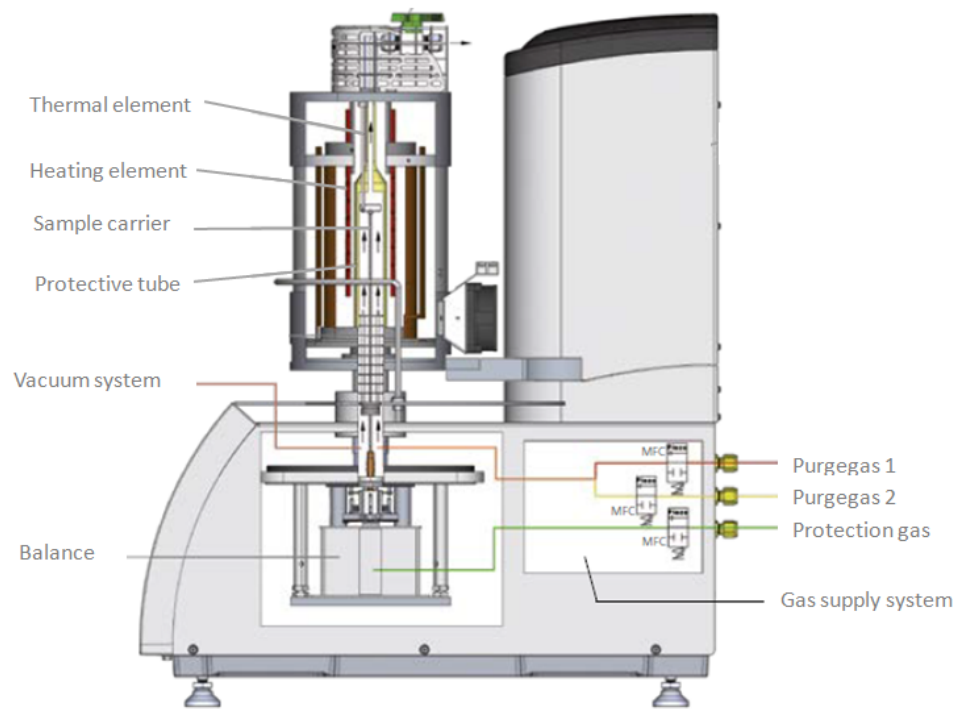
Figure 7: Schematic representation of the STA device, which was used for the investigations in this thesis[18]. The gas supply system with the gas inlets Purgegas 1, Purgegas 2 and Protection gas is responsible for the atmosphere that is used during the measurement. The balance measures the most important information that can be obtained with the STA, namely the mass change during the heat treatment. The vacuum system is required to evacuate the measurement chamber prior to the measurements. The sample is mounted on the sample carrier and the temperature of the measurement chamber is regulated with the heating element.
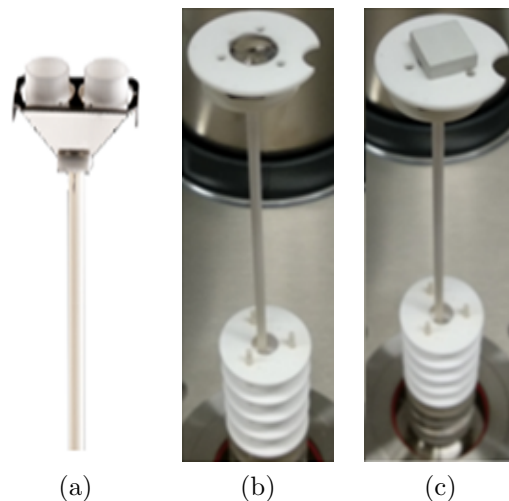
Figure 8: **(a)** Standard DSC sample carrier with two DSC crucibles. **(b)** Sample holder as it was used during the investigation. **(c)** Sample holder as it was used during the investigation + sample.

Combined with the information one can get with the Differential Scanning Calorimetry (DSC), namely the heat flux of a specimen during the measurement, the STA is a potent instrument for the desired investigation of decomposition reactions. Figure 7 shows a schematic representation of the used device. It is called STA 449 F1 Jupiter by the company Netzsch. The DSC information of the TG-DSC measurement was only obtained in the preliminary investigations. For this, small parts of the samples were scraped off (about 40mg) and measured in a standard measurement setup of two crucibles (Figure 8 **(a)**, one of the crucibles contains the sample and one is the empty reference). Due to the size of the final components (between 1080mg and 1180mg, depending on whether it contains an electrode or not), all debinding measurements after the preliminary investigations were carried out in a special setup (Figure 8, **(b)** and **(c)**). Instead of using two crucibles like in standard measurements, the crucibles were removed and a small ceramic plate was used to mount the components. This is possible, because only the TG signal was of interest for the debinding measurements and the DSC signal could be neglected. The detailed settings and values that are used in all measurements are shown in Table 1. Figure 9 shows the measurement device with the final location of the sample holder and the sample.
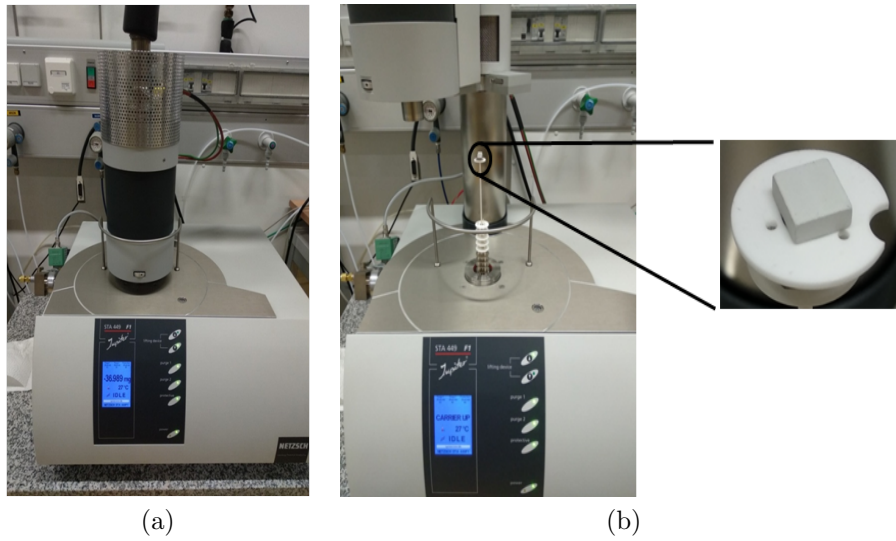
Figure 9: **(a)** STA device with the furnace closed. **(b)** STA device with the furnace opened + magnification of the sample holder with sample.

Table 1: Settings and values of the measurement software, which were used for all experiments.

Paramater	Value
Measurement device	NETZSCH STA 449F1 STA449F1A-0279-M
Mode	DSC-TG
Measurement mode	Sample + Correction
Temperature calibration	TCALZERO.TCX
Sensitivity	SENSZERO.EXX
Crucible	DSC/TG pan Al2O3
DSC/TG pan Al2O3	5000 µV
TG RANGE	5000 mg
Furnace	Sic S
Active furnace position	LEFT
Sample carrier	Sample carrier
Furnace thermal element	S
Sample thermal element	S

2.2.2 MS - Mass Spectrometry

The mass spectrometer is used to identify all substances and reaction products that occur during the debinding process (thermolysis). There are two measurement modes available – the scan mode and the SIM mode (selected ion monitoring). Scan mode means that, depending on the settings of the software, the whole spectrum/range of a mass to charge ratio is recorded. This is suitable for an analysis where it is unknown, which substances are going to be detected or what reaction products could be expected. In contrast to that, the SIM mode is suitable for a permanent monitoring of the emanation of known volatile reaction products. Therefore only specific mass to charge ratios of specific species/ions are detected, which increases the sensitivity of the whole measurement. The mass spectrometer (NETZSCH QMS 403C) was connected to the STA via a capillary like it is shown in Figure 10.

2.2.3 XRD - X-ray Diffraction

The XRD was used to investigate the components after the temperature treatment (debinding process) to identify the solid reaction products. It was carried out with a PANalytical X'Pert Pro diffractometer (Malvern Panalytical Ltd, Malvern, United Kingdom). Cu K-α radiation was used for phase identification and lattice parameter measurements were carried out using HighScore Plus 4.8 software and COD – Crystallography Open Database.

2.3 Oxygen partial pressure

In order to understand the mechanisms of the binder burnout, the measurements were carried out in different atmospheric conditions. Table 2 shows the measurement atmospheres with the corresponding gas flows to meet these settings. Furthermore the resulting oxygen partial pressures are shown in Table 2.

Table 2: Oxygen partial pressures with the required flow rates of the gases to meet the atmospheric conditions.

		Atmosphere					
		0.5% O_2	1% O_2	5% O_2	20 % O_2	N_2	1% H_2, 99% N_2
O_2 p. press.[1]		~ 5	~ 10	~ 50	~ 200	$\sim 10^{-2}$	$\sim 10^{-20}$
	O_2	2	2	5	20	0	0
Gas flow[2]	N_2	398	198	95	80	100	80
	Form. gas[3]	0	0	0	0	0	20

[1] Oxygen partial pressure in [mbar].

[2] Actual gas flow during the measurement in [ml min^{-1}].

[3] Forming gas - 5% H_2, 95% N_2 in the gas bottle.

2.4 Experimental Setup

The final experimental setup is a combination of the STA with the MS as shown in Figure 10. The advantage of this setup is obvious. As soon as a reaction occurs at a specific temperature and a volatile reaction product is formed, this product is detected by the MS (with a small delay). This means that it is possible to identify, which reaction product is formed at what time/temperature.

Figure 10: Final experimental setup with the STA on the right side and the MS on the left side.

3 Results and Discussion

3.1 Preliminary Investigations

Preliminary investigations were the first step to get usable results later on. They were very important in order to gather information about the proper settings of the measurement device (heating rates, maximum temperatures, atmosphere and others) that were used for the complete components in later experiments. It was carried out by scraping off little flakes of the components with a knife. These flakes were then put into a crucible and measured with the respective settings. Examples of these preliminary investigations are shown in Figure 11, Figure 12 and Figure 13.

Figure 11: Results of the preliminary investigations (Flakes of the multilayer component) shown in a mass vs. time diagram.
Settings of the measurement: atmosphere = N_2; heating/cooling rate = 10K/min **(a)** and 1K/min **(b)**; T_{max} = 600°C.

Figure 11 shows that the results of the 10K/min and the 1K/min measurement are very similar. The overall mass loss is about 6%-7% and is more or less reached after 1/3 of the measurement time. This means that a slow heating rate has no advantage in relation to the loss of mass.

Further preliminary investigations were then carried out with other atmosphere settings
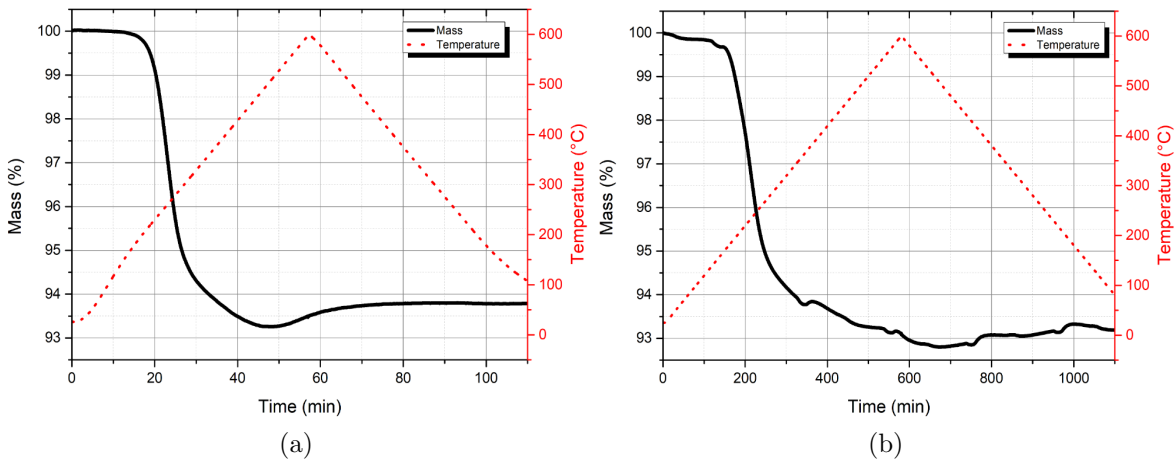
Figure 12: Results of the preliminary investigations (Flakes of the multilayer component) shown in a mass vs. temperature diagram.
Settings of the measurement: atmosphere = N_2; heating/cooling rate = 10K/min **(a)** and 1K/min **(b)**; T_{max} = 600°C.

(e.g.: Synthetic air – 20% O_2, 80% N_2), with the results shown in Figure 13. The mass curves of these measurements are similar to the measurements of the pure N_2 experiment (Figure 11 an Figure 12) but with the difference of a higher mass gain (approximately 0.5% in N_2 and approximately 1% in synthetic air (20% O_2, 80% N_2)) above 400°C. This is assumed to correspond to the oxidation of the inner copper electrode, which is present in the components. Compared to N_2 atmosphere, this reaction is stronger in synthetic air. Because of this, further investigations of the copperpaste, of which the electrodes are made of, were necessary and are discussed in Chapter 3.2.

3.2 Copperpaste

In order to know how the inner copper electrode reacts during the temperature treatment in different atmospheres, the copper paste was measured seperately. The preparation is described in Chapter 2.1.3.1. Figure 14 shows two of these measurements with atmospheres of 5% O_2 (blue) und 0.5% O_2 (green). The heating rate was set to 2K/min and the maximum temperature was set to 650°C.

Even at these low O_2 concentrations one can notice the quite huge mass gain of approximately 20%, which corresponds to the copper oxidation. The small mass loss at the start of the measurement corresponds to residues of the organic additives of the copper paste that were not fully removed during the drying step of the copper paste. It is also
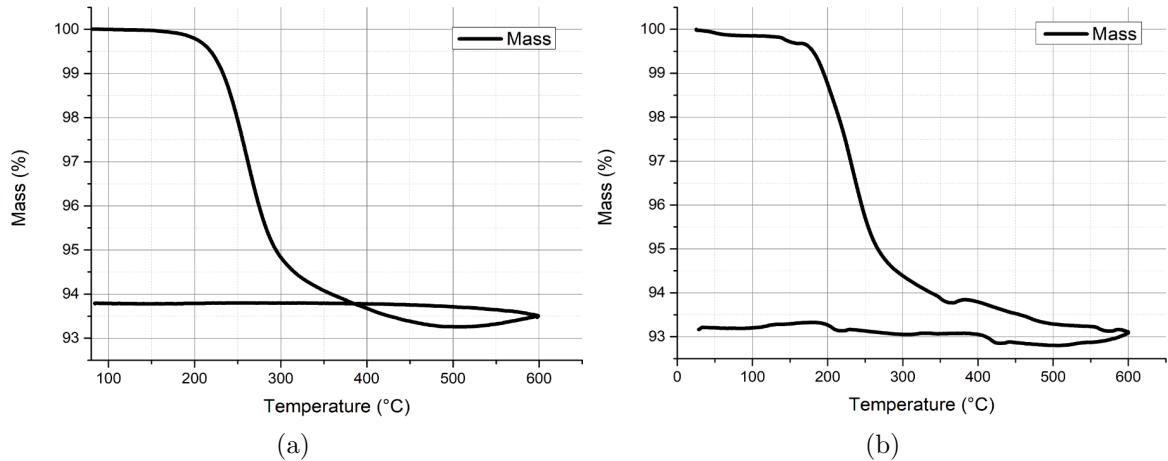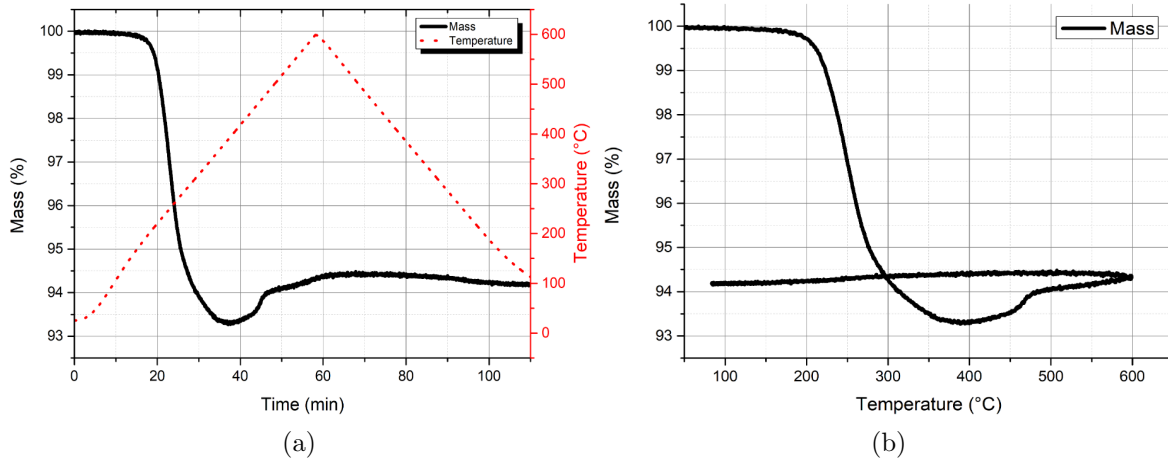
Figure 13: Results of the preliminary investigations (Flakes of the multilayer component) shown in a mass vs. time diagram **(a)** and a mass vs. temperature diagram **(b)**.
Settings of the measurement: atmosphere = Synthetic air (20% O_2, 80% N_2); heating/cooling rate = 10K/min; T_{max} =600°C.

important to notice that the mass increase is not continuous but happens with multiple steps in both cases. This was then further investigated with another measurement (Figure 15). In order to know how the copper paste reacts with different atmospheric conditions, the composition of the atmosphere was changed during the measurement. The results show again a mass gain of about 20%. This increase of the mass happens via multiple steps in a more oxidative atmosphere (N_2/O_2 - 80/20). After about 420°C all the copper is oxidized to copper oxide (CuO) and the maximum mass is reached. At 800°C the atmosphere was changed to a more reducing atmosphere (N_2). This results in a mass loss of approximately 10%, which means that the copper oxidation is reversible to a certain degree. It also indicates the assumption that the copper electrode is at least oxidized to Cu_2O, even in N_2 atmosphere and explains the mass gain of the preliminary investigations, which were measured in N_2. The multiple steps during the mass increase in an oxidative atmosphere are most likely corresponding to the different oxides of copper (Cu_2O and CuO). First the metallic copper is oxidized to Cu_2O and then further oxidized to CuO. This is also mentioned in the literature[19] where very similar results were obtained (Figure 16).

Despite being reversible, the copper oxidation is a crucial point of the whole process and a problem to the mechanical stability of the components. This is discussed in later chapters.
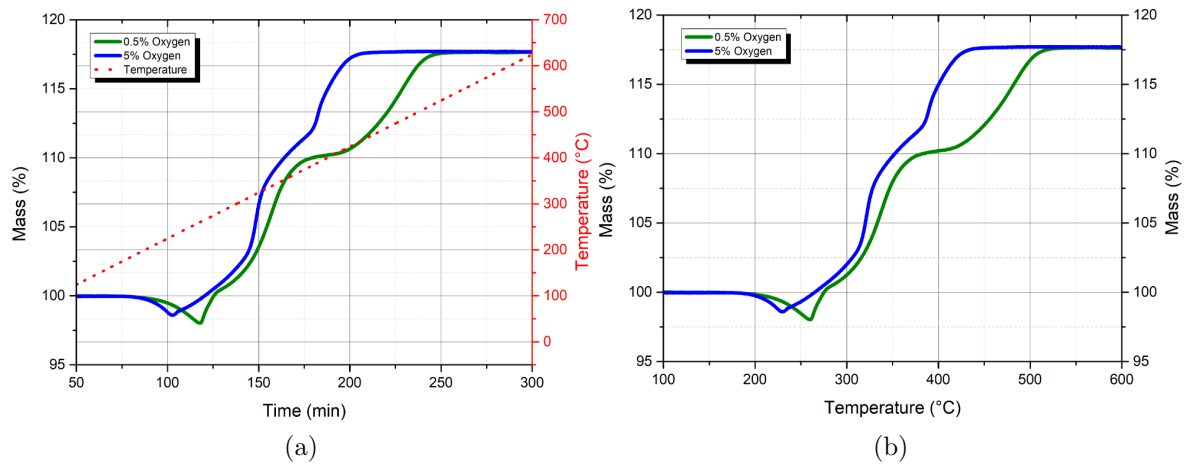
Figure 14: Results of the copper paste measurements shown in a mass vs. time diagram **(a)** and a mass vs. temperature diagram **(b)**.
Settings of the measurement: atmosphere = blue – 5% O_2, 95% N_2; green – 0.5% O_2, 99.5% N_2; heating rate = 2K/min, T_{max} = 650°C.
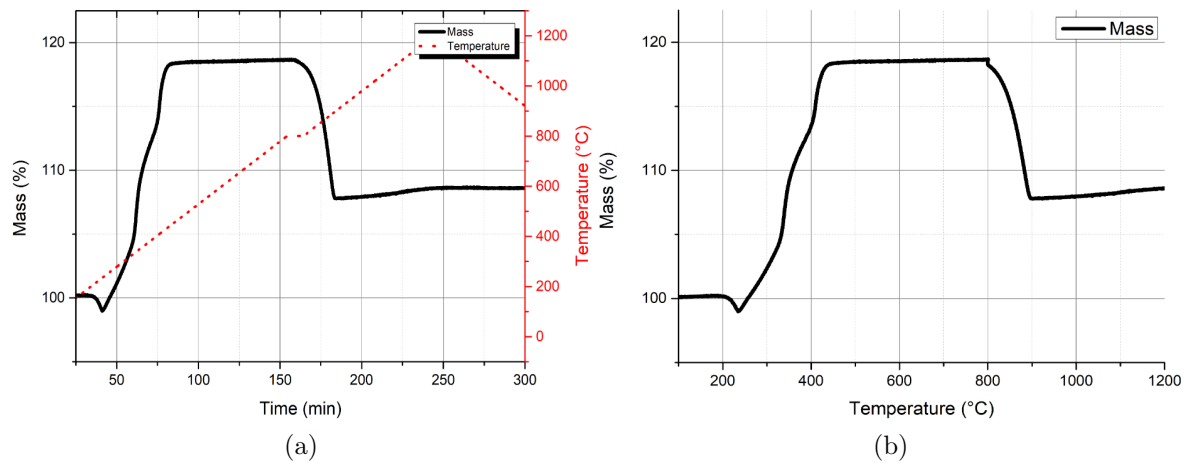
Figure 15: Results of the copper paste measurement with changing atmospheric conditions during the experiment shown in a mass vs. time diagram **(a)** and a mass vs. temperature diagram **(b)**.
Settings of the measurement: atmosphere = 20% O_2, 80% N_2 from 30°C – 800°C and N_2 from 800°C – 1200°C; heating/cooling rate = 5K/min; T_{max} = 1200°C.

20
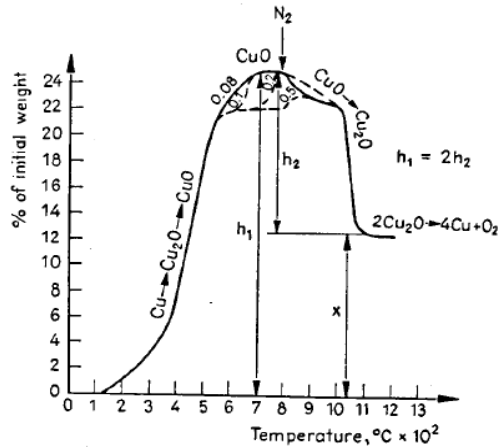
Figure 16: Result of an experiment carried out by A. Lupu in 1970. Metallic copper was first oxidized to CuO via Cu_2O and then reduced back to metallic copper by changing the atmosphere from synthetic air (20% O_2, 80% N_2) to N_2 at a maximum temperature of 800°C[19].

3.3 Components WITHOUT inner electrodes

Due to the results of the preliminary investigations, which showed that there could be problems with the copper oxidation, the measurements were started with components that did not contain an inner electrode. The following results were obtained with measurements that used different atmospheric conditions during the heat treatment.

3.3.1 Atmospheric condition: Synthetic air (20% O_2, 80% N_2)

The results of the measurement in synthetic air are shown in Figure 17. One can see that there is an overall mass loss of about 7%. This corresponds to the total binder content that is present in the component and is burned out during the heat treatment. After about 150 minutes of the measurement there is a rapid, nearly vertical drop of the mass curve and no more mass change is happening whatsoever. Even the isothermic part of the temperature curve has no impact on the mass after this point. At the same time (minute 150) a small peak in the temperature curve is visible. This indicates an overheating, which is due to the strongly exothermic reaction that could not be regulated by the temperature controller. Because of this, the O_2 concentration was reduced for the following experiments.

Figure 17: Results of the measurement of the final component WITHOUT inner electrodes shown in a mass vs. time diagram **(a)** and a mass vs. temperature diagram **(b)**. **Settings of the measurement:** atmosphere = Synthetic air (20% O_2, 80% N_2); heating rate = 2K/min; T_{max} = 650°C with an isothermic gradient at maximum temperature for ten hours.

3.3.2 Atmospheric condition: Reduced oxygen concentration

As mentioned before, the oxygen concentration was reduced in the following experiments. Three different concentrations were chosen, namely 5% O_2, 1% O_2 and 0.5% O_2. Due to the reduced O_2 concentration no additional exothermic reaction is happening and therefore no rapid mass drop and temperature jump is observed in the following results (Figure 18). Like in the 20% O_2 measurement, the overall mass loss of the 5% O_2, 1% O_2 as well as the 0.5% O_2 measurement is about 7%, which indicates that most of the binder is removed in all three cases. Furthermore, at 1% and 0.5% O_2 concentration, the decomposition of the binder occurs in two distinguishable steps with different rates (different gradient from 100%-94.5% compared to 94.5%-93%). The higher the O_2 concentration the faster is the decrease of the mass.

A picture of the component before and after the measurement in synthetic air (20% O_2, 80% N_2) is shown in Figure 19. The green body **(a)**, which has a greyish color, is completely white afterwards **(b)**. This, namely a nearly completely binder free ceramic part that is ready for further processing, is the desired result for the components that contain an inner electrode. This is possible in the measurements that were just mentioned, because the inner copper electrode is missing in these components. However, with the knowledge of the preliminary investigations it is going to be very difficult to archive this goal without damaging the final component (with copper electrode) due
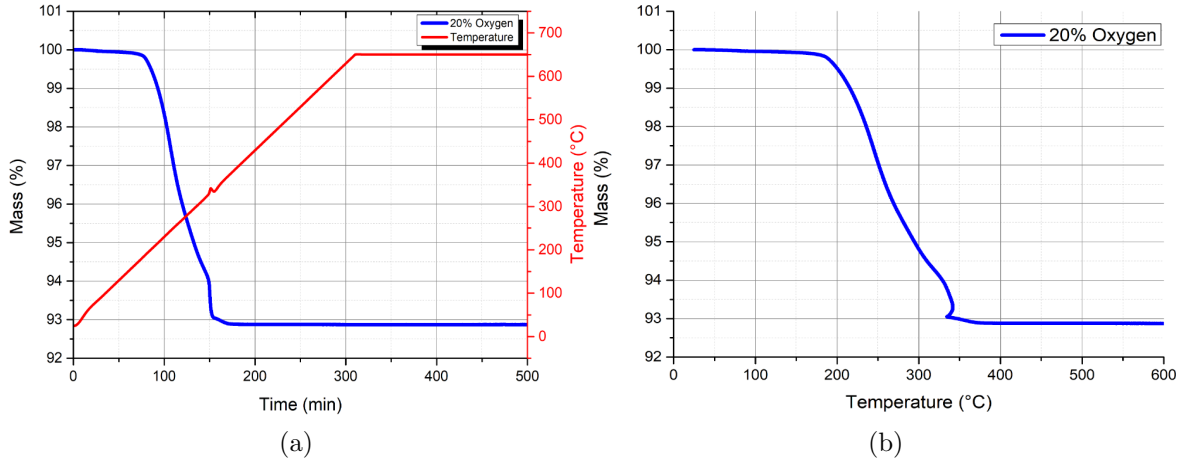
Figure 18: Results of the measurement of the final component WITHOUT inner electrodes shown in a mass vs. time diagram **(a)** and a mass vs. temperature diagram **(b)**. **Settings of the measurement:** atmosphere = blue – 5% O_2, 95% N_2, purple – 1% O_2, 99% N_2, green – 0.5% O_2, 99.5% N_2; heating rate = 2K/min; T_{max} = 650°C with an isothermic gradient at maximum temperature for ten hours.

to copper oxidation and consequently mechanical failure of the parts. Because of this reason, other atmospheric conditions were used in the following measurements.

Due to the problem of copper oxidation even in reduced O_2 atmosphere, the atmospheric conditions were changed again. The idea was to reduce the oxygen partial pressure even further. This was achieved by using N_2 in one experiment (oxygen partial pressure ~10^{-5}bar) and forming gas (= mixture of 1% H_2 and 99% N_2; oxygen partial pressure ~10^{-23}bar) in another. Figure 20 shows the results of these measurements. The first feature to notice is that in both cases the overall mass loss is higher than the 7% mass loss of the measurements in 20% O_2, 5% O_2, 1% O_2 and 0.5% O_2 atmosphere. This

Figure 19: Components WITHOUT inner electrodes before **(a)** and after **(b)** the measurement in synthetic air (20% O_2, 80% N_2).
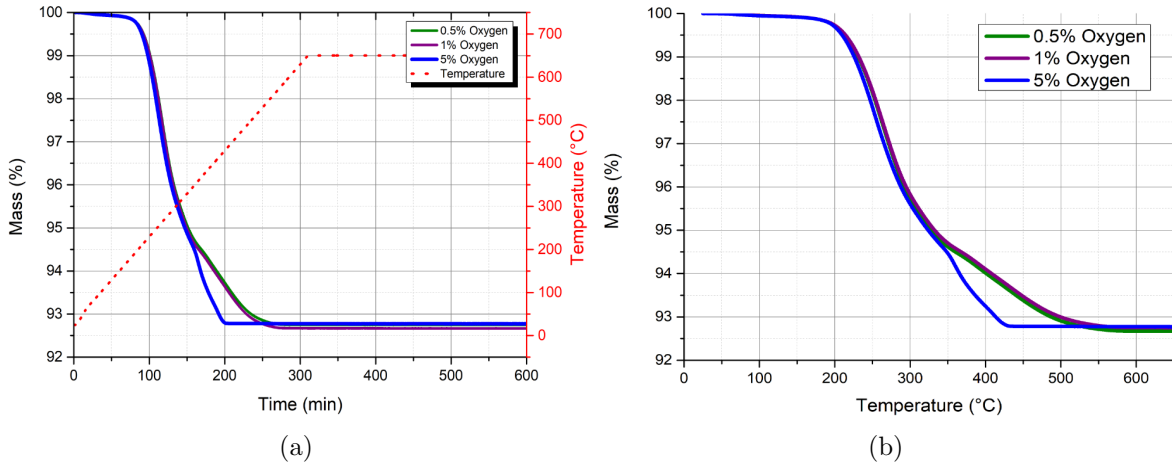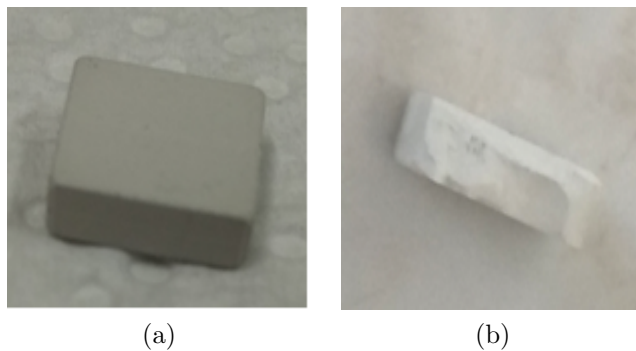
23
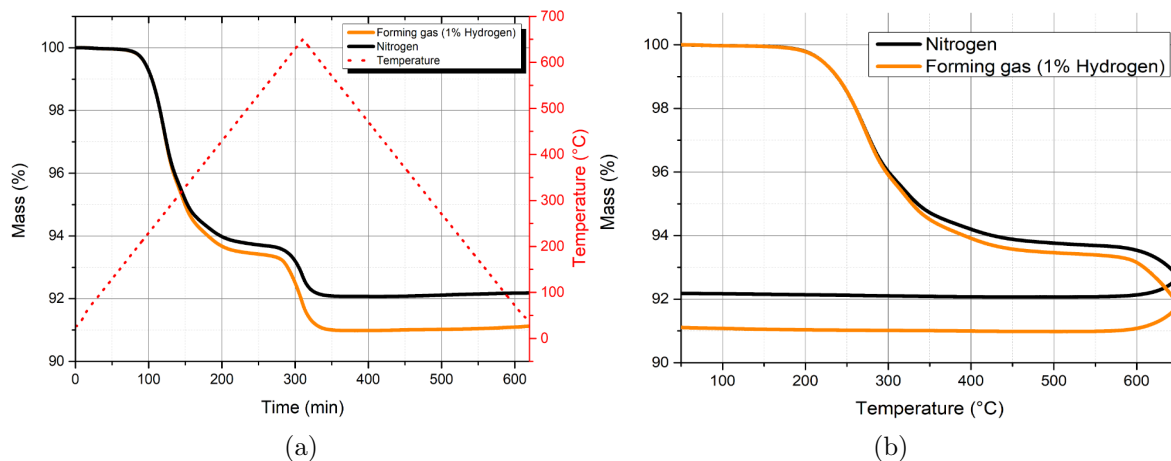
Figure 20: Results of the measurement of the final component WITHOUT inner electrodes shown in a mass vs. time diagram **(a)** and a mass vs. temperature diagram **(b)**. **Settings of the measurement:** atmosphere = black – N_2, orange – Forming gas (1% H_2/99%N_2); heating/cooling rate = 2K/min; T_{max} = 650°C.

means that in addition to the mass loss that is caused by the decomposition of the organic binder, another reaction that leads to the additional 1% mass loss in the case of N_2 atmosphere and the additional 2% mass loss in the case of forming gas, occurs. Other constituents of the component (e.g. the ceramic material) must be responsible for this additional mass loss. Furthermore it is a two step mass loss, which also supports the assumption that there are two reactions responsible for the mass loss in the more "reducing" atmospheres N_2 and forming gas.

Because of the coupling with a mass spectrometer it was possible to continuously record a mass spectrum (in scan mode to detect all incoming mass fragments) during the STA measurement. Therefore it was possible to get information about the decomposition products that were released from the components during the heat treatment at a specific time and temperature. Figure 21 shows such a mass spectrum of the measurement in N_2. Part **(a)** was measured at 277°C, which corresponds to the first step of the mass loss. Part **(b)** was measured at 646°C, which corresponds to the second step of the mass loss. The most important differences of these two spectra are the peaks between the masses 36-45, 50-57, and 69-73. The masses 36-45 are most likely C3-fragments, the masses 50-57 C4-fragments and the masses 69-73 are C5-fragments. These fragments are generated during the thermal decomposition of the organic components (binder, plasticizer, etc.) and are only present in the spectrum taken at 277°C. In the case of the 646°C measurement (second step) all of these fragments are missing or at very low

24

intensities. This means that most of the binder is removed from the component at this point. However, the first step of the mass loss does not reach the 7% mass loss that were obtained with the measurement in synthetic air. This means that there is some residual carbon left, which is evidenced by the black color of the components (Figure 22 and Figure 23). Most of the mass decrease of the second step comes from the mass fragment 44 (CO_2). It has a much higher intensity at 646°C and is generated by the reaction of carbon monoxide (CO) with other constituents of the ceramic component (=reduction), which leads to the additional mass loss. The CO itself is generated by the reaction of residual carbon in an atmosphere with a deficiency of O_2 (discussed in more detail in Chapter 1.3.2). The resulting reaction products of these side reactions are discussed in Chapter 3.3.4 for the components WITHOUT inner electrodes and in Chapter 3.4.3 for the components WITH inner electrodes.

(a)   (b)
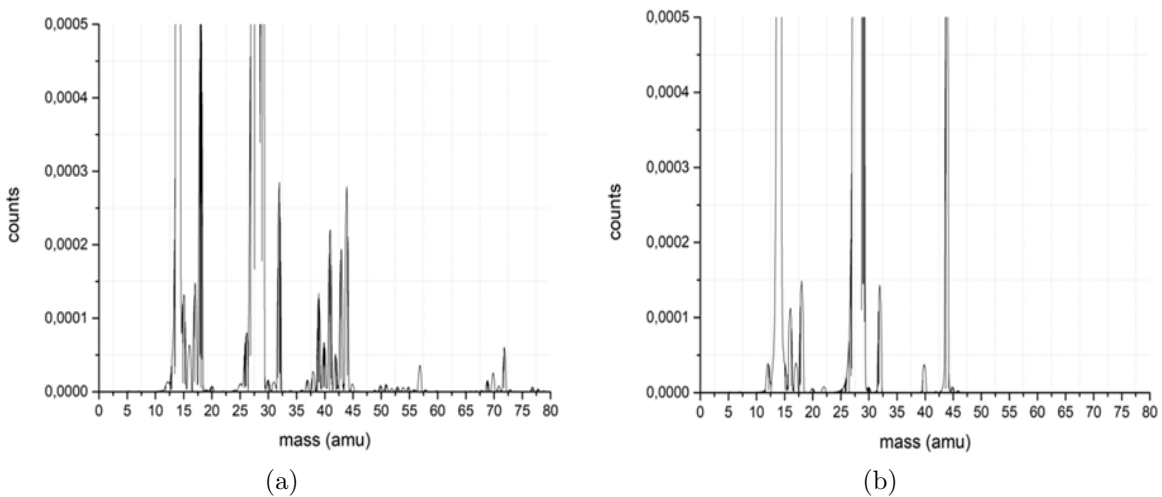
Figure 21: Mass spectra (scan mode) of the measurement of the final components WITHOUT inner electrodes in N_2. **(a)** at 277°C, **(b)** at 646°C.

Figure 22 and Figure 23 show how the components are affected by the different gases. In the case of forming gas (Figure 22) the whole component changed its color from greyish to black. This result is undesired for a subsequent sintering process.

In the case of N_2 atmosphere (Figure 23) the color of the component changed from greyish to white (only on the surface). What was firstly thought a success and positive result, turned out to be as negative as the result with forming gas. After making a cross-section of the component, the - again - completely black inside of the parts was observed.
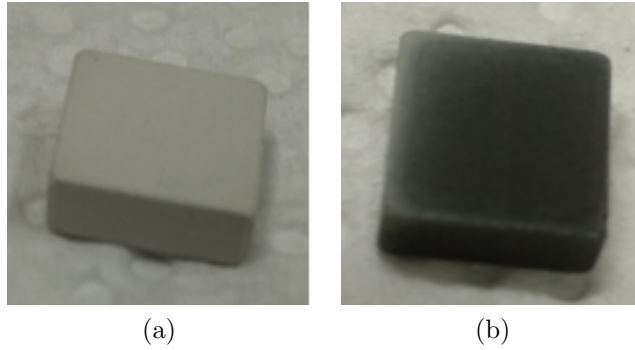
Figure 22: Components WITHOUT inner electrodes before **(a)** and after **(b)** the measurement in forming gas (1% H_2/99% N_2).
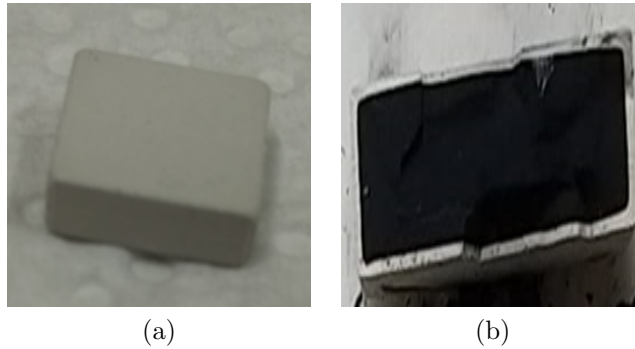
Figure 23: Components WITHOUT inner electrodes before **(a)** and after **(b)** the measurement in N_2.

3.3.3 Comparison and summary of the different atmospheric conditions

A comparison and summary of the results of the different atmospheric conditions is shown in Figure 24. One can clearly see that the measurement with the 5% O_2 atmosphere shows the lowest mass loss, because the decrease of the mass is only affected by the binder burnout. The lower the oxygen content in the atmosphere gets, the more side reactions are happening and the higher the mass loss becomes (7% O_2, 8% in N_2 and 9% in forming gas).

Figure 24: Comparison of the measurement of the final component WITHOUT inner electrodes shown in a mass vs. time diagram **(a)** and a mass vs. temperature diagram **(b)**. **Settings of the measurement:** atmosphere = blue – 5% O_2, 95% N_2, black – N_2; orange - Forming gas (1% H_2/99%N_2); heating/cooling rate = 2K/min; T_{max} = 650°C.

3.3.4 XRD analysis

The results of the XRD analysis are shown in Figure 25. The peaks at 21,5°, 31°, 38° and 44° show the perovskite structure of the PLZT. Reaction products that were formed during the heat treatment are indicated with green and blue arrows at the respective reflection. The only measurement that shows these side reaction products is the N_2 experiment. Due to the reduced oxygen partial pressure (appr. 10^{-5}bar) the ceramic material (Lanthanum doped Lead Zirconate Titanate) is decomposed to PbO, Pb and/or ZrO_2. Those side reaction products are indicated with green (28,5° and 32°) and blue (31° and 36°) arrows. Because of their very similar diffraction pattern, Pb and ZrO_2 are hard to distinguish. The small peaks at 24,5° 34° and 40° of the measurement in N_2 could not be identified.

3.4 Components WITH inner electrodes

Finally, after the preliminary investigations and the study of the components without inner electrodes, the components with inner electrodes were investigated. Again the effect of oxygen in different concentrations was investigated to find out how the inner copper electrodes react inside the whole component during the heat treatment. Due to the reasons that were already discussed in Chapter 3.3.1 (exothermic reaction due to

27
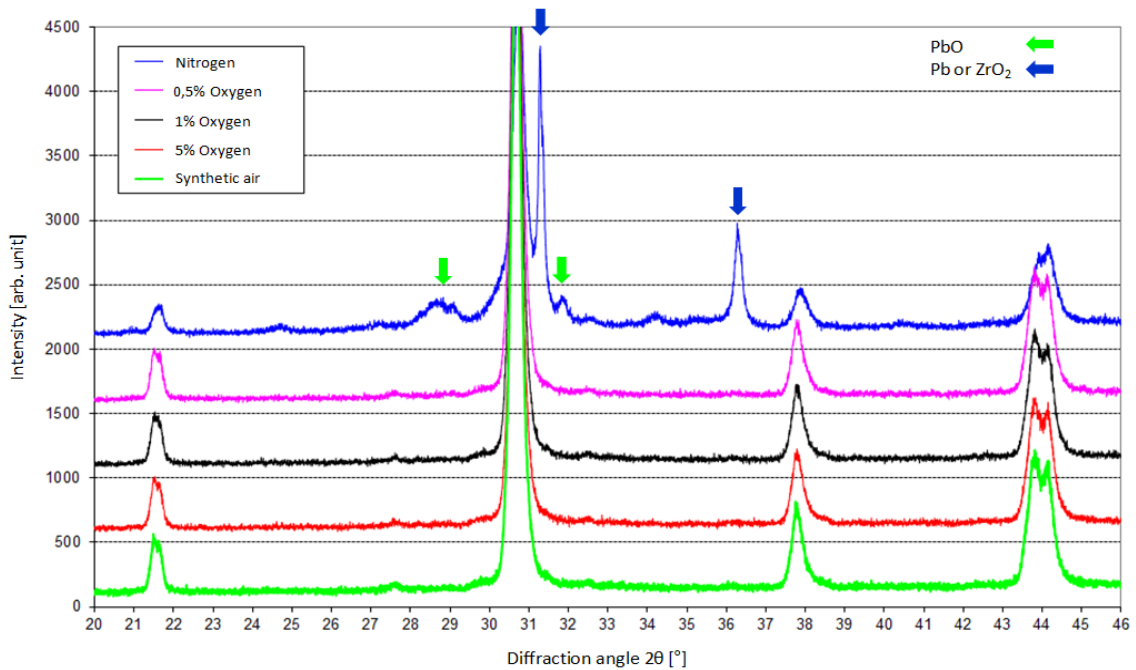
Figure 25: Results of the XRD analysis of the components WITHOUT inner electrodes with the atmospheric conditions of the respective measurement in the top left corner of the figure. The green (PbO) and blue (Pb or ZrO_2) arrows at the respective angles indicate the side reaction products that were formed during the heat treatment.

high O_2 concentration), the measurement in synthetic air (20% O_2, 80% N_2) was not carried out with the components that contain inner electrodes. Instead, the experiments were carried out in already reduced oxygen concentrations.

3.4.1 Atmospheric condition: Reduced oxygen concentration

Like in the measurements of the components without inner electrodes, O_2 concentrations of 5%, 1% and 0.5% were chosen for these experiments. The results are shown in Figure 26. It stands out that the 0.5% O_2 and the 1% O_2 measurements are rather similar and show a two step mass loss, while the 5% O_2 measurement is quite different to the other two and only shows a one step mass loss. However, all three measurements show that there is a problem with copper oxidation, which leads to a mass increase and overlaps the mass loss that is happening due to binder burnout. Only the 0.5% O_2 measurement (green in Figure 26) reached the 7% mark of the mass loss, which was obtained in the measurements without the electrodes and corresponds to the total binder content. However, the sample then again started to increase its mass due to the copper oxidation
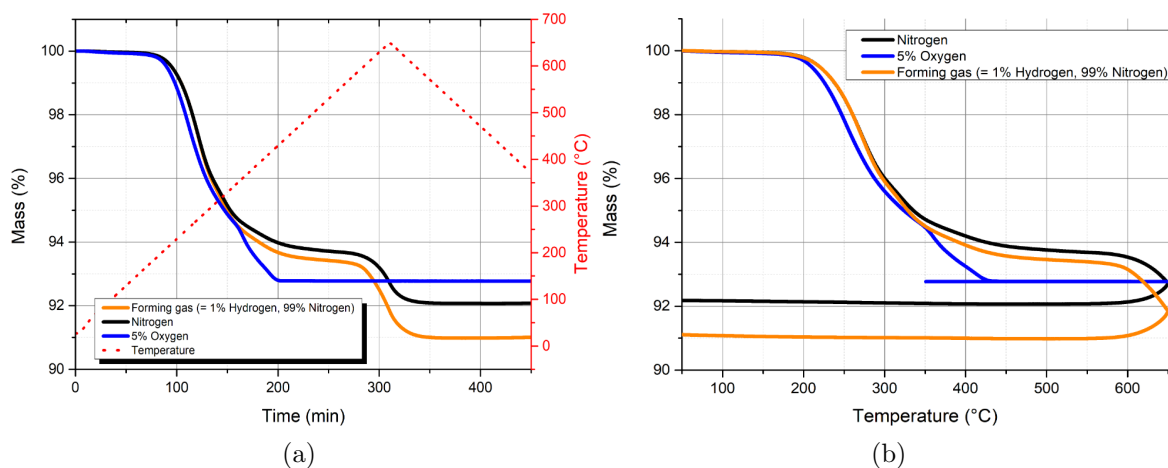
Figure 26: Results of the measurement of the final component WITH inner electrodes shown in a mass vs. time diagram **(a)** and a mass vs. temperature diagram **(b)**.
Settings of the measurement: atmosphere = blue – 5% O_2, 95% N_2, purple – 1% O_2, 99% N_2, green – 0.5% O_2, 99.5% N_2; heating rate = 2K/min; T_{max} = 650°C.
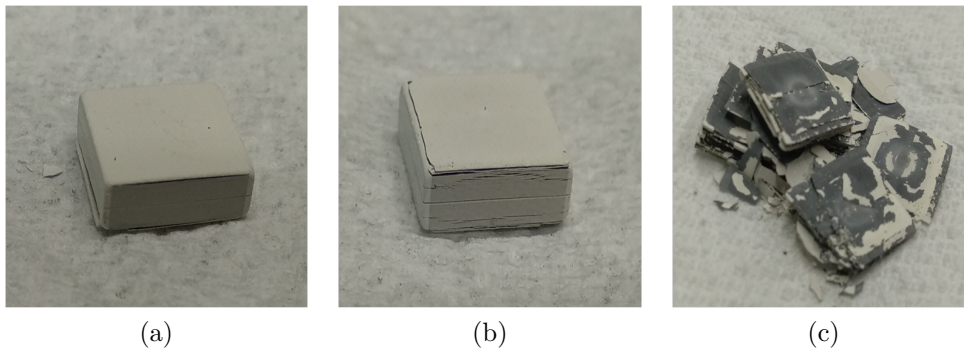
Figure 27: Components WITH inner electrodes after the measurement in 0.5% O_2 **(a)**, 1% O_2 **(b)** and 5% O_2 **(c)**.

of the inner electrode. The 5% O_2 measurement (blue in Figure 26) shows a mass loss of about 6% followed by a mass gain of 1% due to the copper oxidation. In the case of the 5% O_2 measurement it is also worth to mention that, due to the high oxygen partial pressure and therefore the fast oxidation of the inner electrode, only one step of the mass loss could be observed. Images of the ceramic parts after the heat treatment are shown in Figure 27. One can see that the components were delaminated in all three cases. This is most obvious in the 5% O_2 measurement, where the part is completely delaminated. Due to the volume expansion that is caused by the copper oxidation the mechanical stress for the parts is too high to withstand a mechanical failure. The higher the oxygen content in the atmosphere, the higher is the damage to the components.
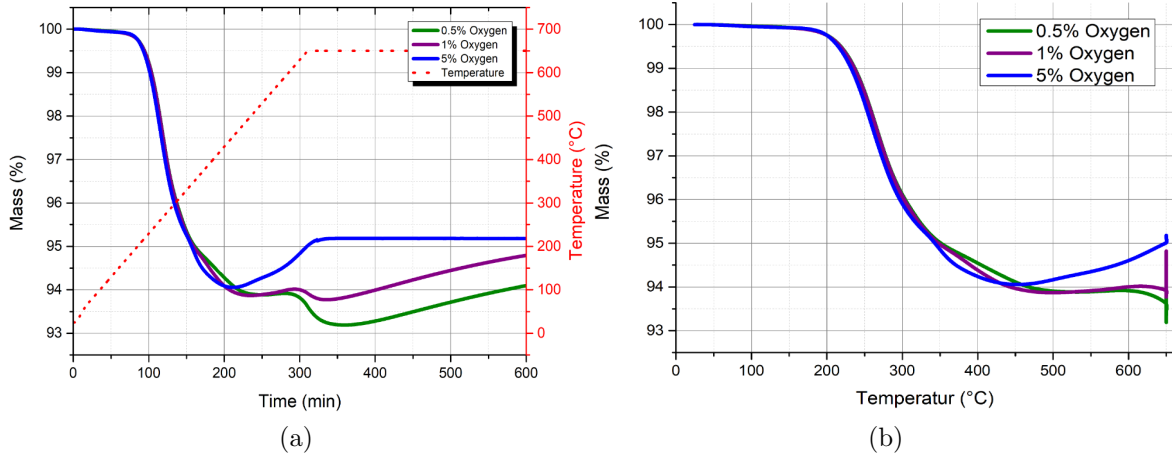
Figure 28: Results of the measurement of the final component WITH inner electrodes shown in a mass vs. time diagram **(a)** and a mass vs. temperature diagram **(b)**.
Settings of the measurement: atmosphere = blue – 5% O_2, 95% N_2, purple – 1% O_2, 99% N_2, green – 0.5% O_2, 99.5% N_2; heating rate = 2K/min; T_{max} = 650°C.
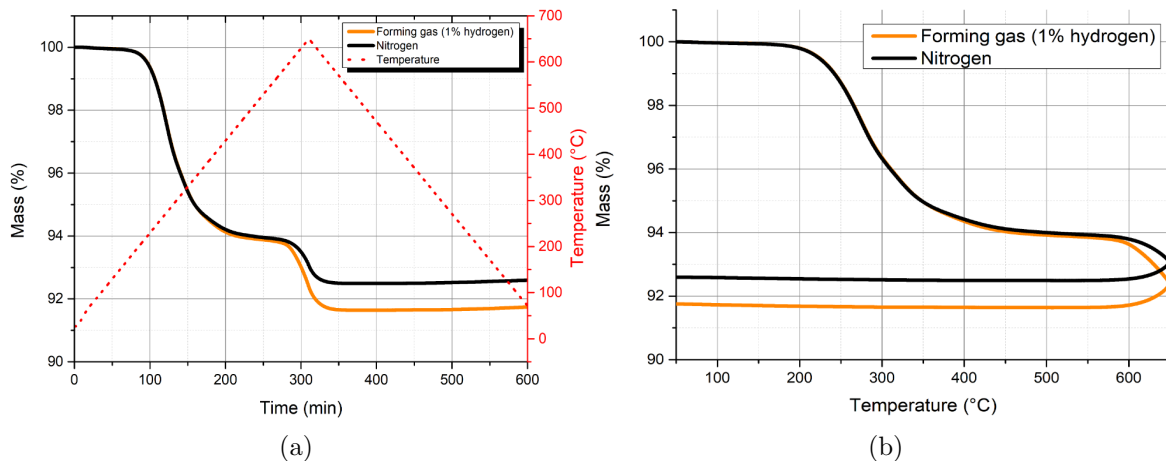
Because of the damage that is done to the components when measured in 5%, 1% and 0.5% O_2, the oxygen partial pressure was further reduced by using N_2 and/or forming gas (1% H_2, 99% N_2). The results of these measurements (Figure 28) are very similar to the results of the measurements shown in Chapter 3.3.2 (Figure 20 - without electrodes). There is a two step mass decrease with the second step only existing when using N_2 and/or forming gas atmosphere.

Figure 29 shows an image of the part after the heat treatment. Again, one can clearly see the delaminated layers within the component, which means it is damaged and cannot be used for further processing. The sample of the forming gas measurements looked exactly the same as the sample of the measurement without inner electrodes (Figure 22).

The information that was obtained with the MS in scan-mode, namely what mass fragments are formed at which specific time and temperature respectively, was now used to select specific mass fragments, which were then measured with the MS in SIM-mode. This allowed to keep track of the specific mass fragments that were generated at each of the two mass decease steps. The following Figures 30-32 show the results of the STA measurements in N_2 atmosphere overlayed with the MS SIM-mode measurements.

In Figure 30 the occurrence of water during the first and the second mass loss step is indicated by the mass fragments 18 (H_2O^+) and 17 (OH^+).

The result of the SIM-mode measurement shown in Figure 31 further confirms what
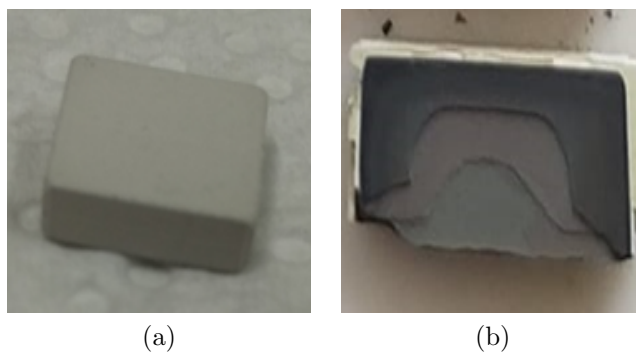
(a)   (b)

Figure 29: Components WITH inner electrodes before **(a)** and after **(b)** the measurement in N_2.

Figure 30: Results of the STA measurements of the final component WITH inner electrodes in N_2 atmosphere (black) overlayed with the SIM-mode MS measurements of the mass fragments 18 und 17 (dark blue and bright blue respectively).

Figure 31: Results of the STA measurements of the final component WITH inner electrodes in N_2 atmosphere (black) overlayed with the SIM-mode MS measurements of the mass fragments 72 and 57 (dark green and bright green respectively).

is already shown in the scan-mode MS measurement (Figure 21). The first mass loss at about 300°C mainly corresponds to carbonchain fragments (e.g.: 72 – C5 fragment (dark green), 57 – C4 fragment (bright green)) that are generated during the thermolysis of the binder. They are only detected during the first mass loss step and are missing in the second step (650°C). This means that the binder burnout is mostly completed after the first step.

The same applies to the yellow graph in Figure 32. The mass fragment 43 is only detected within the first mass loss step and missing in the second step. It corresponds to a carbon fragments that is only generated during the binder burnout. However, the fragment with the mass 44 (CO_2^+) is present during both mass loss steps. It contributes a small amount to the first step but is most responsible for the second one, which is caused by reduction of the ceramic material. The mechanism and reaction products are discussed in more detail in Chapter 3.4.3.

3.4.2 Modification of the atmospheric conditions

Because of the problems that are mentioned in earlier chapters, namely that the material is either damaged by copper oxidation in O_2 atmosphere or by reduction of the ceramic material in a more reductive atmosphere (N_2 or forming gas), it was attempted to
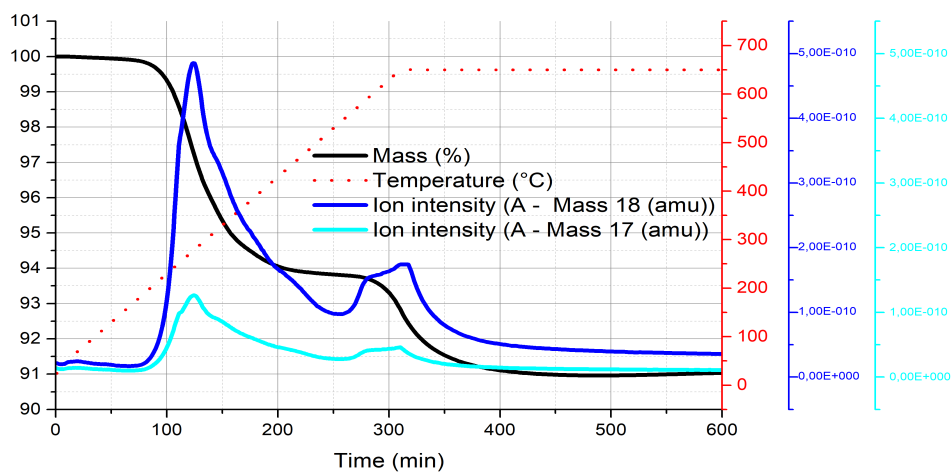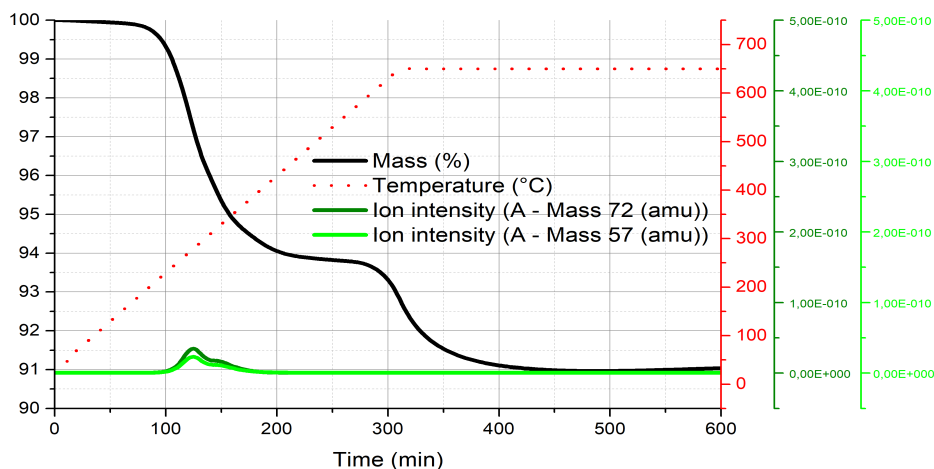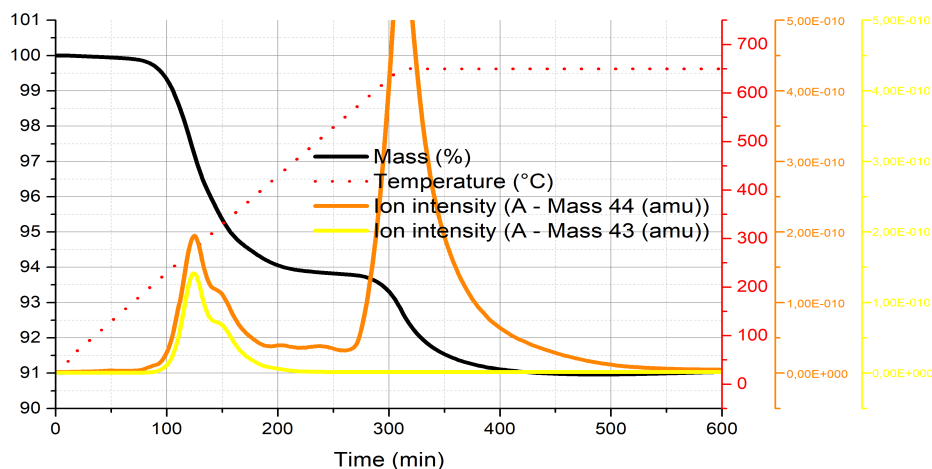
Figure 32: Results of the STA measurements of the final component WITH inner electrodes in N_2 atmosphere (black) overlayed with the SIM-mode MS measurements of the mass fragments 44 and 43 (orange and yellow respectively).

modify the temperature- and atmosphere settings, in order to avoid these side reactions. The exact settings of the following measurements are listed in Table 3 and the results are shown in Figure 33. The idea was to start in pure N_2 atmosphere and then only heat to the specific temperature where the first mass step (binder burnout) is mostly finished, but the second one (reduction of the ceramic material) has not started yet. This temperature is about 450°C (Figure 28 **(b)**) and it was then maintained for 1h to try to ensure the completion of step one. After that the sample was cooled down to room temperature and the atmosphere was changed to 1% O_2 at that point. However, due to the copper oxidation that starts at approximately 450°C (Figure 26 **(b)**) the maximum temperature in O_2 atmosphere was set to 350°C. This temperature was then maintained for 5h and should finally ensure that all residual binder is properly removed. Figure 33 shows that after 1h at 450°C in N_2 atmosphere the binder burnout is not totally completed. Only 6% mass loss are reached instead of the 7% total binder content. In the following segment after the change to 1% O_2 atmosphere, a mass increase of about 0.5% is noticeable and the expected 7% total mass loss are not reached either. This means that the copper electrodes are again oxidized and therefore the parts are damaged. For a closer look at what is actually happening during the different temperature- and atmosphere segments, a SIM-mode MS measurement was recorded simultaneously to the STA measurement. The results are shown in Figures 34-36. Ad-

Table 3: Temperature- and atmosphere profile of the modified measurement.

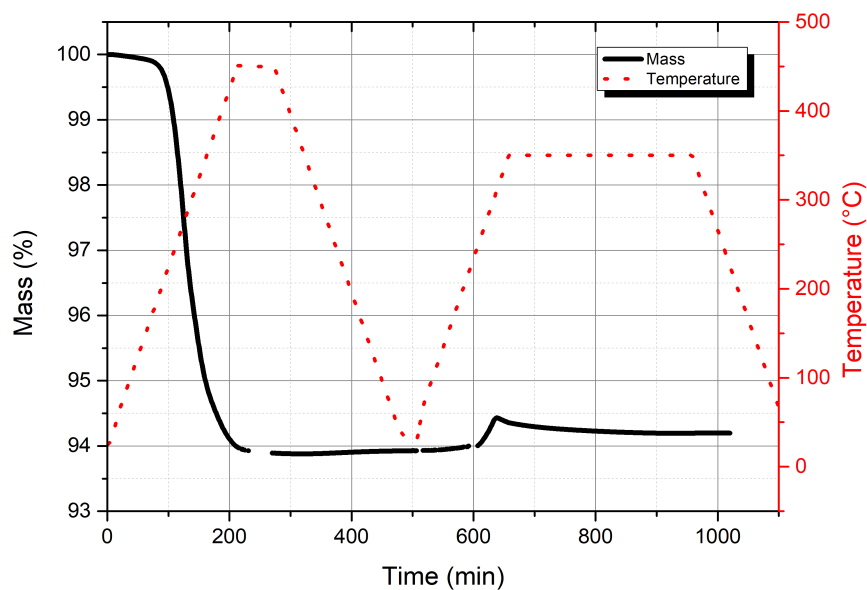| Temperature	Atmosphere
start at 25°C	N_2
heating rate 2K/min until 450°C	N_2
1h at 450°C	N_2
cooling rate 2K/min until 25°C	N_2
at 25°C	change to 1% O_2
heating rate 2K/min until 350°C	1% O_2
5h at 350°C	1% O_2
cooling rate 2K/min until 25°C	1% O_2

Figure 33: Results of the measurement of the final component WITH inner electrodes with modified temperature- and atmosphere settings (settings are shown in Table 3).
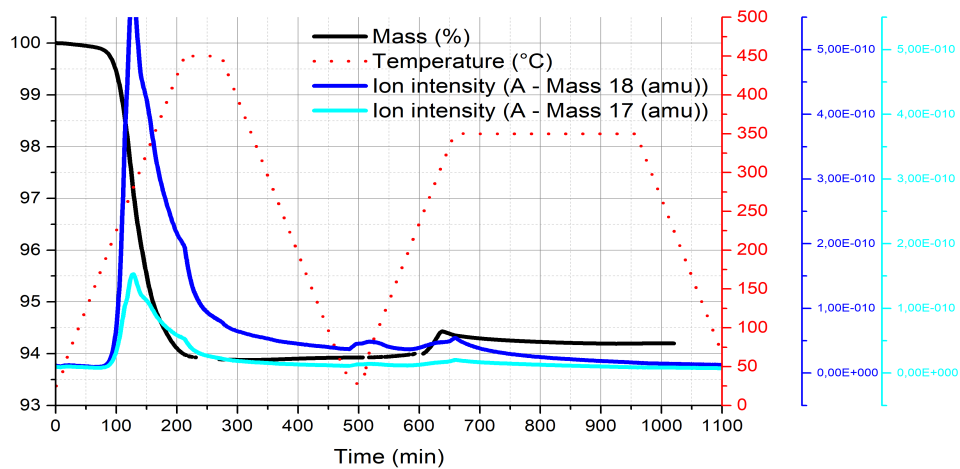
Figure 34: Results of the STA measurements of the final component WITH inner electrodes in the modified temperature- and atmosphere settings (black) overlayed with the SIM-mode MS measurements of the mass fragments 18 and 17 (dark blue and bright blue respectively).

ditionally, an XRD analysis was carried out to investigate whether the ceramic material was decomposed (see Chapter 3.4.3, Figure 38).

Figure 34 shows again the occurrence of water during the heat treatment. It is indicated by the mass fragments 18 (H_2O^+) and 17 (OH^+). Figure 35 shows that, despite the lower maximum temperature in order to prevent the reduction of the material, the process causes the decomposition of the binder into larger fragments. The C-fragments (72 and 57) are only detected during the first mass loss step as in the measurement with pure N_2 atmosphere (Figure 31). This means that most of the binder burnout must be completed. However, due to the fact that only 6% mass loss is obtained instead of 7%, it can be assumed that residual carbon is left inside the components, which should be removed in the second mass loss step. This actually should have been prevented by the use of the modified temperature- and atmosphere profiles.

The peak of the mass fragment 43 (C3-fragment) in Figure 36 shows what was expected. It is only present during the first mass loss step (binder burnout) and not existing after that. With a closer look on the mass fragment 44 (CO_2), one can notice that the intensity of the first peak is about the same compared to the measurement in pure N_2 (Figure 32). However, this first peak corresponds to the binder burnout and not to the reduction, which does not start until about 600°C (Figure 28 (**b**)). The second peak of

35

Figure 35: Results of the STA measurements of the final component WITH inner electrodes in the modified temperature- and atmosphere settings (black) overlayed with the SIM-mode MS measurements of the mass fragments 72 and 57 (dark green and bright green respectively).
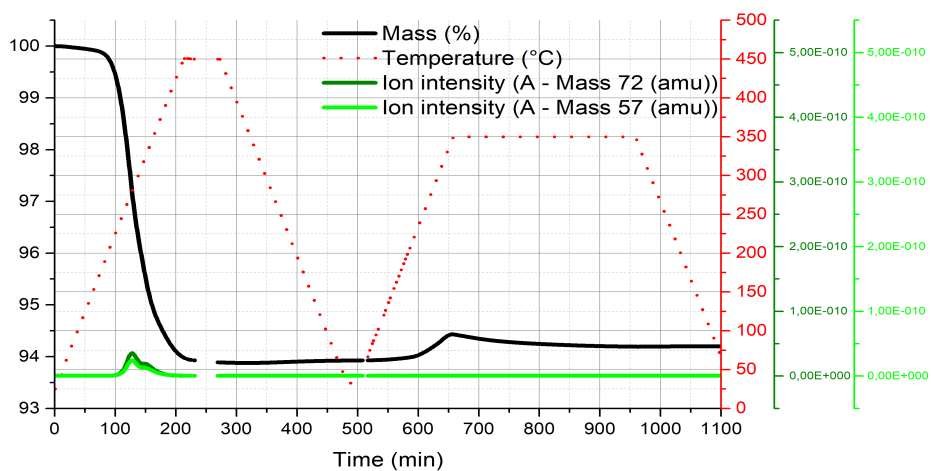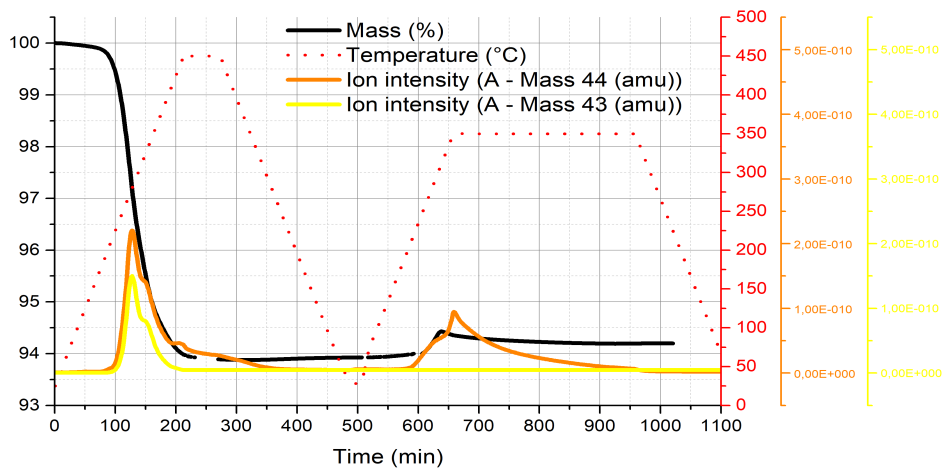

Figure 36: Results of the STA measurements of the final component WITH inner electrodes in the modified temperature- and atmosphere settings (black) overlayed with the SIM-mode MS measurements of the mass fragments 44 and 43 (orange and yellow respectively).

Figure 37: Components WITH inner electrodes after the measurement with modified temperature- and atmosphere settings.

the fragment 44 (CO_2, in Figure 36) has a much lower intensity compared to the same peak in Figure 32 (pure N_2 measurement). Because of this it can be assumed, that the reduction/decomposition is prevented for the most part when using the modified settings. Figure 37, which shows the ceramic parts after the treatment in the modified temperature- and atmosphere settings, confirms this assumption. The parts are mostly white and not completely black like in the measurement in pure N_2 (Figure 29). The increase of the mass after the change to 1% O_2 atmosphere indicates the oxidation of the copper. Despite lowering the maximum temperature from 650°C to 350°C in O_2 atmosphere, the very low concentration of O_2 (and therefore low oxygen partial pressure) is sufficient to oxidize the inner copper electrode, which damages the ceramic parts. Figure 37 shows the delaminated components.

3.4.3 XRD analysis

An XRD analysis of the components with inner electrodes was carried out after the treatment in different atmospheres (N_2, 5% O_2, 0.5% O_2 and the modified settings measurement). The results are shown and compared in Figure 38. As mentioned in Chapter 3.3.4 the peaks at 21,5°, 31°, 38° and 44° in Figure 38 show the perovskite structure of the PLZT. The green graph represents the measurement of the component without inner electrode in synthetic air. It is used as a reference to compare the other measurements with, as no side reactions were observed in this specific experiment. The orange arrows (32,5°, 35,5° and 39°) show CuO, which evidences the occurence of the copper oxidation side reaction. It is only observed in the 5% O_2 and 0.5% O_2 measurement and not present in the N_2 measurement and in the measurement with modified settings. Decomposition of the ceramic material to PbO, Pb and ZrO_2 can be observed in the N_2 and the 0.5% O_2 measurement and the reaction products are

indicated with blue (31° and 36°) and green (28,5° and 32°) arrows. In the case of the 0.5% O_2 measurement this is an interesting difference compared to the measurement of the components without inner electrodes. There, no decomposition of the material was observed in the 0.5% O_2 measurement. This can be due to the reason that copper acts as an oxygen getter and thus locally decreases the oxygen partial pressure to a value where a decomposition of the material is happening. The decomposition of the ceramic material in general happens due to the reaction with carbon monoxide (CO), which is itself generated from residual carbon in a low oxygen partial pressure atmosphere. CO is oxidized to CO_2 and a reduction and furthermore decomposition of PLZT to Pb, PbO and ZrO_2 is the consequence.

The results of the XRD analysis show that the modified settings measurement (black graph in Figure 38) is the most promising one. No decomposition of the ceramic material can be observed in this case whatsoever. Furthermore, no CuO is found, which means that the copper oxidation is prevented to a large extend. However, the red arrows at 36,5° and 42° show Cu_2O. This means that the change of the atmospheric conditions as well as the lower temperature during the measurement successfully inhibits the oxidation of the copper electrode to a higher oxidation state. However, it is not prevented completely and therefore damage is done to the components nevertheless (Figure 37).
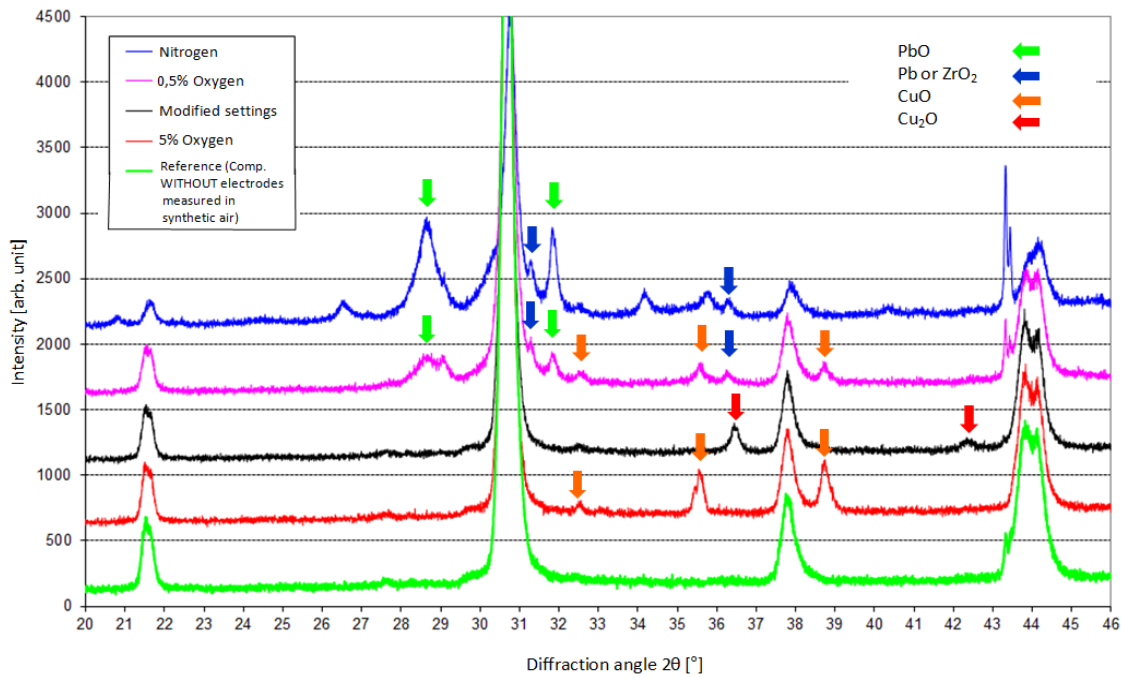
Figure 38: Results of the XRD analysis of the components WITH inner electrodes with the atmospheric conditions of the respective measurement in the top left corner of the figure (green graph shows the reference = component without inner electrodes measured in synthetic air). The green (PbO), orange (CuO), blue (Pb or ZrO_2) and red (Cu_2O) arrows at the respective angles indicate the undesired side reaction products that were formed during the heat treatment.

3.5 Comparison and summary

In the following section the measurements of the ceramic parts with and without an inner electrode are compared. There is only one atmospheric condition where a significant difference between these two could be observed. The other two give similar results.

3.5.1 Atmospheric condition: N_2

Figure 39: Comparison of the results of the measurement of the final component WITHOUT inner electrodes (grey) and WITH inner electrodes (black) shown in a mass vs. time diagram **(a)** and a mass vs. temperature diagram **(b)**.
Settings of the measurement: atmosphere = N_2; heating/cooling rate = 2K/min; T_{max} = 650°C.

Figure 39 shows the comparison of the two different parts in N_2 atmosphere. It stands out that there is no significant difference in the mass profile. The only thing one can notice is that the part without electrodes loses about 0.5% more weight than the part with electrodes. However, this is due to the fact that the parts containing inner electrodes are heavier overall but lose less weight percentagewise, because the copper electrode contains less binder that could be burned out.

3.5.2 Atmospheric condition: Forming gas (1% H_2 / 99% N_2)

What was valid for the comparison of the measurements in N_2 is also true for forming gas (Figure 40). However, a slightly higher mass loss can be observed in the forming gas measurement because of the lower oxygen partial pressure and therefore a further
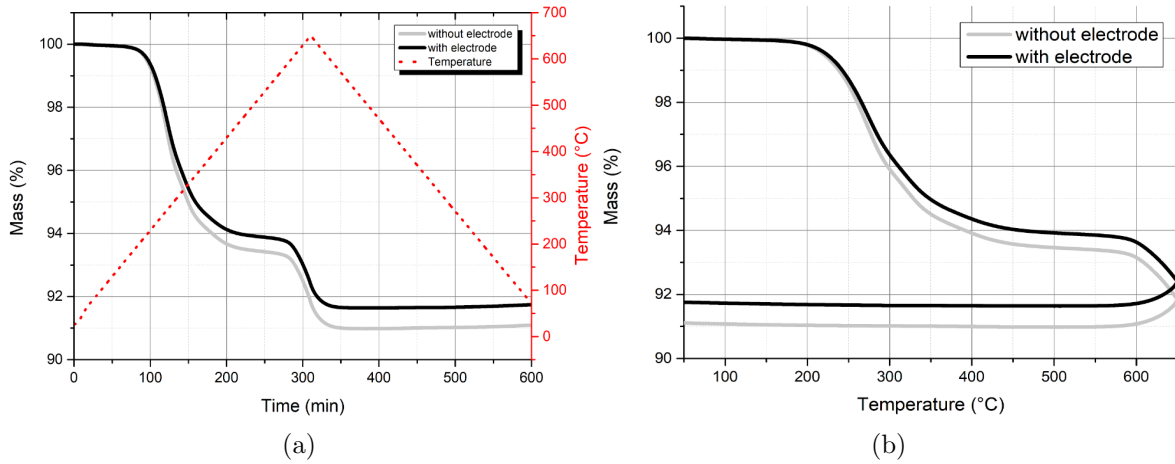
Figure 40: Comparison of the results of the measurement of the final component WITHOUT inner electrodes (grey) and WITH inner electrodes (black) shown in a mass vs. time diagram **(a)** and a mass vs. temperature diagram **(b)**.
Settings of the measurement: atmosphere = forming gas (1% H_2/$99\%N_2$); heating/cooling rate = 2K/min; T_{max} = 650°C.

reduction/decomposition of the ceramic material. Otherwise there is no significant difference whatsoever. The higher mass loss of the parts without electrodes is already explained in the N_2 case.
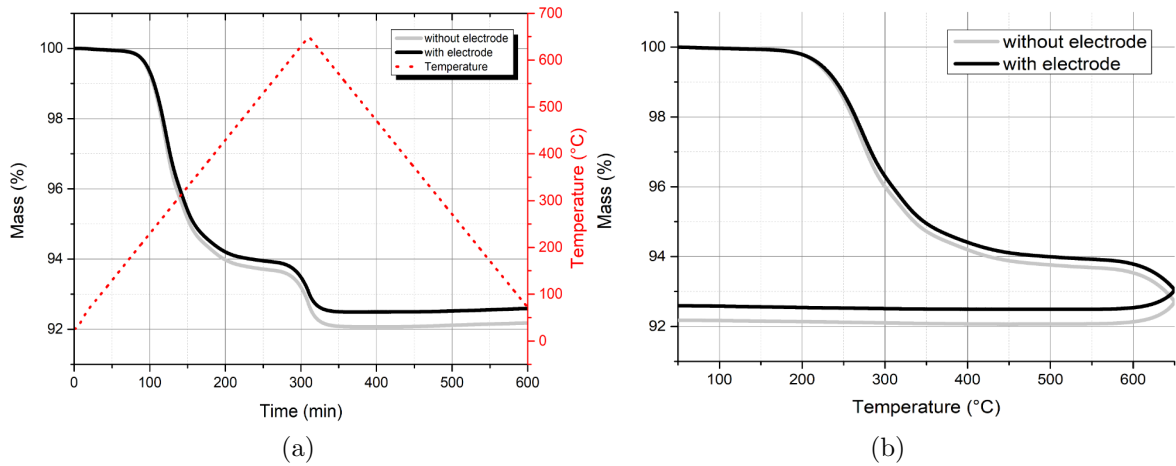
3.5.3 Atmospheric condition: 5% O_2
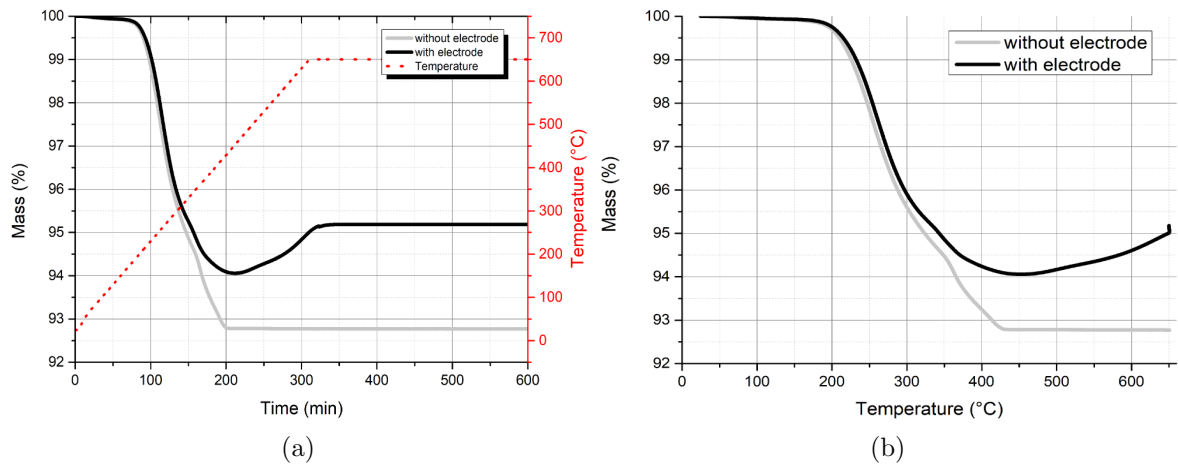
Figure 41: Comparison of the results of the measurement of the final component WITHOUT inner electrodes (grey) and WITH inner electrodes (black) shown in a mass vs. time diagram **(a)** and a mass vs. temperature diagram **(b)**.
Settings of the measurement: atmosphere = 5% O_2, 95% N_2; heating/cooling rate = 2K/min; T_{max} = 650°C.

The atmospheres containing 5%, 1% and 0.5% O_2 cause significant differences between the two parts. The 5% O_2 measurement was chosen as an example and is shown in Figure 41. While there is no oxidation of the inner copper electrode in N_2 atmosphere and a mass loss of about 7% is obtained, the copper is oxidized in 5% O_2 atmosphere and the mass is increasing again after a certain threshold as a consequence.

4 Conclusion

The debinding process of the "green" Multilayer Ceramic Capacitors (MLCC) is a very complex process with a lot of different reaction mechanisms behind it and a lot of variables that have to be considered. The most important of those variables is the atmosphere or in more detail, the oxygen partial pressure during the debinding process. It determines whether the components can be used in applications afterwards or if they are damaged during the debinding process and therefore must be sorted out.

The preliminary investigations with TG-DSC measurements were helpful to get a rough idea of the reactivity of the components in different measurement atmospheres. However, no valid statement of the real components could be made with the preliminary investigations alone. Therefore the final components with and without inner electrodes were investigated more closely.

In the case of the components that do not contain inner electrodes, the thermolysis (binder burnout) in O_2 atmosphere (5%, 1% and 0.5% O_2) worked out well. The total binder content of the components ($\sim$7%) was obtained as a mass loss after a reasonable time of about 3-4h. The XRD analysis showed no decomposition reaction of the ceramic material whatsoever in all three cases, which is further evidenced by the completely white appearance of the component. However, by changing the measurement atmosphere to a lower oxygen partial pressure (N_2 and/or forming gas), the mass loss proceeded in two steps and exceeded the 7% that was observed in the 5%, 1% and 0.5% O_2 experiment (8% in N_2 and 9% in forming gas). The mass spectrum showed that, depending on the temperature and time, different reaction products were obtained. The first mass loss step happens between 200°C-500°C and corresponds mostly to side chain fragments that are cleaved off the binder molecules during the thermolysis. The second one happens after 500°C, generates mostly CO_2 and is assumed to correspond to a reduction/decomposition reaction of the ceramic material (PLZT). The XRD analysis confirms this as Pb, PbO and ZrO_2 were found. It can be assumed that residual carbon (mainly from the backbone of the polymeric binder) generates carbon monoxide (CO) inside the components in an atmosphere with a low oxygen partial pressure. This is evidenced by the black appearance of the components after the measurement in low

oxygen partial pressure atmospheres. The CO then reacts with the constituents of the ceramic material, forms CO_2 and decomposes the Lanthanum doped Lead Zirconate Titanate (PLZT) to e.g. metallic Pb, PbO and/or ZrO_2. This leads to a higher mass loss than the $\sim$7% total binder content.

The measurement in atmospheres containing 5%, 1% and 0.5% O_2, that delivered good results when using the components without inner electrodes, revealed problems when using the components that contain inner electrodes. No matter which oxygen concentration was used during the measurements, the results showed a mass loss followed by a mass increase. This is most probably due to the copper oxidation of the inner electrodes, which was evidenced by the XRD analysis, where CuO was found. Further evidence for the copper oxidation and therefore volume expansion of the inner electrode is the appearance of the components after the measurement. The higher the O_2 concentration during the measurement the further delaminated are the parts. The measurements in more reducing atmospheres (N_2 and/or forming gas) showed similar results as the measurement of the components without inner electrodes in the same atmospheres. Again, a two step mass loss was observed with the first step happening between 200°C-500°C and the second step after 500°C with an overall mass loss of 7.5% and 8.5% in N_2 and forming gas respectively. The mass spectrum, which was recorded simultaneously to the STA measurement, showed that the first step indeed corresponds to the cleavage of the binder molecules and the second step happens mostly due to evolving CO_2 as a consequence of a decomposition reaction. This is evidenced by the XRD analysis, where Pb, PbO and ZrO_2 was found in low oxygen partial pressure atmospheres (e.g. N_2). The black appearance of the components after the measurement confirms this further. It is interesting to notice that in the case of the 0.5% O_2 measurement, where no decomposition of the ceramic material was observed when using the components without electrodes, a small amount of decomposition was observed when using components that contain electrodes. This is assumed to be the case, because copper acts as an oxygen getter and decreases the local oxygen partial pressure to a value where the decomposition can take place.

Because of the problems that were mentioned before, a measurement with the modified settings was carried out. The idea was that a lower temperature during the measurement together with a change of the atmosphere at a specific time should prevent the oxidation of the copper electrodes as well as the reduction/decomposition reaction of the ceramic material.

The STA measurement of this experiment showed that despite the N_2 atmosphere at the

start, only one mass loss step of about 6% was observed. This means that the second mass loss step, which mainly corresponds to the decomposition of the ceramic material was prevented. This is evidenced by the mass spectrum where a much lower amount of CO_2 was observed, by the XRD analysis where no decomposition products (Pb, PbO and ZrO_2) were found and finally by the appearance of the component itself (mostly white as in the 5%, 1% and 0.5% O_2 measurement). The 1% residual binder to reach the 7% total binder content should have been removed after the change of the atmosphere to 1% O_2. However, despite the lower temperature and the low oxygen concentration (1%) the copper oxidation proceeded and led to a mass increase of about 0.5%. This is evidenced by the XRD analysis where Cu_2O was found and by the delaminated components. However, this is an improvement compared to the measurements in 5%, 1% and 0.5% O_2 atmosphere as the oxidation stopped at the lower oxidation state of copper (Cu_2O - Cu^+ vs. CuO - Cu^{2+}).

At this point it can be stated that no "sweet-spot" could be found with the used process conditions. The components are damaged either by the oxidation of the copper electrode or by the decomposition reaction of the ceramic material.

46

Bibliography

[1] Ming-Jen Pan & Clive A. Randall. *A Brief Introduction to Ceramic Capacitors.* IEEE Electrical Insulation Magazine; Volume 26, p. 44-55, 10th June 2010.

[2] Jinglei Li et al. *Multilayer Lead-Free Ceramic Capacitors with Ultrahigh Energy Density and Efficiency.* Adv. Mater., 30, 1802155, 2018.

[3] James S. Reed. *Principles of Ceramics Processing.* 2nd Edition, p. 583-624 (Chapter 29).

[4] Wenxu Jia et al. *Advances in lead-free high-temperature dielectric materials for ceramic capacitor application.* IET Nanodielectrics 1 (1), April 2018.

[5] Sharath Sriram & Madhu Bhaskaran & Arnan Mitchell. *Piezoelectric thin film deposition: novel self-assembled island structures and low temperature processes on silicon.* Sciyo, 1st chapter of "Piezoelectric Ceramics" p. 1, edited by Ernesto Suaste Gómez.

[6] Nikolay Mukhin et al. *Microstructure and Properties of PZT Films with Different PbO Content - Ionic Mechanism of Built-In Fields Formation.* Materials, 12, 2926, 2019.

[7] A. Mayeen & N. Kalarikkal. *Development of ceramic-controlled piezoelectric devices for biomedical applications.* 2nd chapter of "Fundamental Biomaterials: Ceramics" p. 48, edited by Sabu Thomas, Preetha Balakrishnan, M. S. Sreekala.

[8] M. Jabbari et al. *Ceramic tape casting: A review of current methods and trends with emphasis on rheological behaviour and flow analysis.* Materials Science and Engineering B, 212, 39-61, 2016.

[9] James S. Reed. *Principles of Ceramics Processing.* 2nd Edition, p. 525-534 (Chapter 26).

[10] D. Hotza & P. Greil. *Review: aqueous tape casting of ceramic powders.* Materials Science and Engineering A202, 206-217, 1995.

[11] K. Hong et al. *Perspectives and challenges in multilayer ceramic capacitor for next generation electronics.* J. Mater. Chem. C, 7, 9782-9802, 2019.

[12] Vishwa N. Shukla & David C. Hill. *Binder Evolution from Powder Compacts: Thermal Profile for Injection-Molded Articles.* J. Am. Ceram. Soc., 72 [10] 1797-803, 1989.

[13] Ravi K. Enneti & Seang Jun Park & Randall M. German. *Review: Thermal Debinding Process in Particulate Materials Processing.* Materials and Manufacturing Processes, 27:2, 103-118, 2012.

[14] Kuen-Shan Jaw & Chung-King Hsu & Jinn-Shinng Lee. *The thermal decomposition behaviours of stearic acid, paraffin wax and polyvinyl butyral.* Thermochimica Acta, 367-368, 165-168, 2001.

[15] Laurence W. McKeen. *Permeability Properties of Plastics and Elastomers (Fourth Edition).* p. 181, 2017.

[16] Allen D. Godwin. *Plasticizers.* Elsevier, 9th chapter of "Applied Polymer Science 21st Century", p. 165, edited by Clara D. Craver, Charles E. Carraher, Jr.

[17] Robert F. Speyer. *Thermal Analysis of Materials.* School of Materials Science and Engineering, Georgia Institute of Technology, Atlanta, Geogia, p. 111-124.

[18] NETZSCH. *Simultane Thermische Analyse - STA 449 F1 Jupiter.* Brochure, S. 9, 10.

[19] A. Lupu. *Thermogravimetry of copper and copper oxides (Cu_2O-CuO).* Journal of Thermal Analysis, Vol. 2, 445-458, 1970.